Article

Immunity

Liver-Resident NK Cells Control Antiviral Activity of Hepatic T Cells via the PD-1-PD-L1 Axis

Graphical Abstract

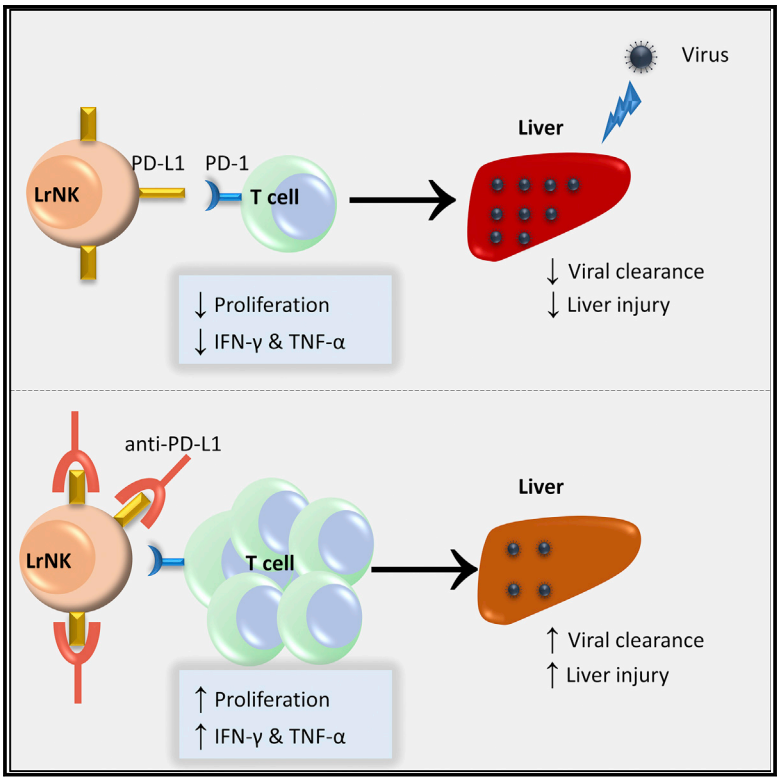

Highlights

- Expression of negative immune-regulatory genes is enriched in LrNK cells
- Virus-specific T cell responses are enhanced in LrNK-cell-deficient mice
- LrNK cell transfer inhibits hepatic T cell responses against LCMV and adenoviruses
- Blockade of PD-L1 abrogates the inhibitory effect of LrNK cells on T cells

Authors

Jing Zhou, Hui Peng, Kun Li, ..., Haiming Wei, Rui Sun, Zhigang Tian

Correspondence

huipeng@mail.ustc.edu.cn (H.P.), tzg@ustc.edu.cn (Z.T.)

In Brief

Zhou et al. find that during viral infection, liver-resident NK (LrNK) cells inhibit the function of hepatic T cells via PD-1-PD-L1 interactions. Their findings reveal a role for LrNK cells in the regulation of T cell immunity and provide insight into the mechanisms of immune tolerance in the liver.

Zhou et al., 2019, Immunity *50*, 403–417
February 19, 2019
https://doi.org/10.1016/j.immuni.2018.12.024

CellPress

Immunity
Article

Liver-Resident NK Cells Control Antiviral Activity of Hepatic T Cells via the PD-1-PD-L1 Axis

Jing Zhou,[1,2] Hui Peng,[1,2,*] Kun Li,[1] Kun Qu,[1] Baohui Wang,[1,2] Yuzhang Wu,[3] Lilin Ye,[3] Zhongjun Dong,[4] Haiming Wei,[1,2] Rui Sun,[1,2] and Zhigang Tian[1,2,5,*]
[1]Division of Molecular Medicine, Hefei National Laboratory for Physical Sciences at Microscale, CAS Key Laboratory of Innate Immunity and Chronic Disease, School of Life Sciences, University of Science and Technology of China, Hefei, Anhui 230027, China
[2]Institue of Immunology, University of Science and Technology of China, Hefei, Anhui 230027, China
[3]Institute of Immunology, Third Military Medical University, Chongqing 400038, China
[4]School of Medicine, Tsinghua University, Beijing 100086, China
[5]Lead Contact
*Correspondence: huipeng@mail.ustc.edu.cn (H.P.), tzg@ustc.edu.cn (Z.T.)
https://doi.org/10.1016/j.immuni.2018.12.024

SUMMARY

The tolerogenic microenvironment of the liver is associated with impaired hepatic T cell function. Here, we examined the contribution of liver-resident natural killer (LrNK) cells, a prominent hepatic NK cell compartment, to T cell antiviral responses in the liver. The number of virus-specific T cells increased in LrNK-cell-deficient mice during both acute and chronic lymphocytic choriomeningitis virus infection. Upon infection with adenovirus, hepatic T cells from these mice produced more cytokines, which was accompanied by reduced viral loads. Transfer of LrNK cells into LrNK-cell-deficient or wild-type mice inhibited hepatic T cell function, resulting in impaired viral clearance, whereas transfer of conventional NK cells promoted T cell antiviral responses. LrNK-cell-mediated inhibition of T cell function was dependent on the PD-1-PD-L1 axis. Our findings reveal a role for LrNK cells in the regulation of T cell immunity and provide insight into the mechanisms of immune tolerance in the liver.

INTRODUCTION

Natural killer (NK) cells are important innate effectors, serving as a first line of defense against pathogens via direct cytotoxicity and the production of various cytokines (Vivier et al., 2008). NK cells are also endowed with immune-regulatory functions through interactions with T cells, B cells, and dendritic cells (DCs), thus contributing to the shaping of the adaptive immune responses (Lam and Lanier, 2017; Schuster et al., 2016; Zhang et al., 2006). NK cells can promote the differentiation of Th1 cells by secreting interferon-γ (IFN-γ) (Laouar et al., 2005; Martín-Fontecha et al., 2004), and they can induce maturation of DCs and enhance their co-stimulatory roles (Adam et al., 2005; Gerosa et al., 2002; Mocikat et al., 2003). NK cells also exert negative regulatory roles on T cell responses through direct and indirect mechanisms. NK cells can secrete interleukin-10 (IL-10) to inhibit $CD4^+$ and $CD8^+$ T cell responses (Deniz et al., 2008; Lee et al., 2009; Mehrotra et al., 1998) or directly kill $CD4^+$ and $CD8^+$ T cells (Cerboni et al., 2007; Rabinovich et al., 2003; Waggoner et al., 2011). In addition, NK cells can eliminate DCs and thereby negatively regulate T cell responses (Cook and Whitmire, 2013). NK cells are now considered a heterogeneous population with phenotypically and functionally distinct subsets (Seillet et al., 2016; Spits et al., 2016). However, the respective roles of the different NK cell subsets remain undefined.

Recently, we and others identified a unique subset of NK cells enriched in the murine liver, which we described as $CD49a^+$ $CD49b^-$ liver-resident NK (LrNK) cells (Peng et al., 2013; Sojka et al., 2014). LrNK cells and conventional NK (cNK) cells exhibit significant differences in terms of phenotype, gene expression profile, and roles in contact hypersensitivity (Peng et al., 2013; Peng and Tian, 2017; Tang et al., 2016; Weizman et al., 2017). Moreover, compared with cNK cells, LrNK cells require different transcription factors and progenitor origins for their development (Constantinides et al., 2014; Klose et al., 2014; Mackay et al., 2016; Zhang et al., 2016). Therefore, LrNK cells represent a distinct cell lineage in the innate lymphoid cell (ILC) family and are also referred to as liver ILC1s to distinguish them from cNK cells. Although knowledge of this NK cell population is increasing, there are still many questions concerning the specific functional properties of the cells (Peng and Sun, 2017; Peng et al., 2016). LrNK cells rapidly produce IFN-γ at sites of primary viral infection and thereby limit early murine cytomegalovirus (MCMV) replication (Weizman et al., 2017). However, it remains unknown whether, and to what extent, LrNK cells contribute to subsequent adaptive immune responses during viral infections.

Immune responses in the liver are generally associated with the induction of tolerance (Crispe, 2009). Administration of antigens via the portal vein can efficiently induce antigen-specific tolerance (Limmer et al., 2000), and allogeneic liver transplants that are incompatible with major histocompatibility complex (MHC) are readily accepted without the need for immunosuppression (Cunningham et al., 2013; Tiegs and Lohse, 2010). Hepatitis viruses, such as hepatitis B virus (HBV) and hepatitis C virus (HCV), can exploit the immunosuppressive liver microenvironment to establish life-long viral persistence (Protzer et al., 2012). The tolerogenic microenvironment of the liver is associated with impaired T cell responses (Crispe, 2009; Tiegs and

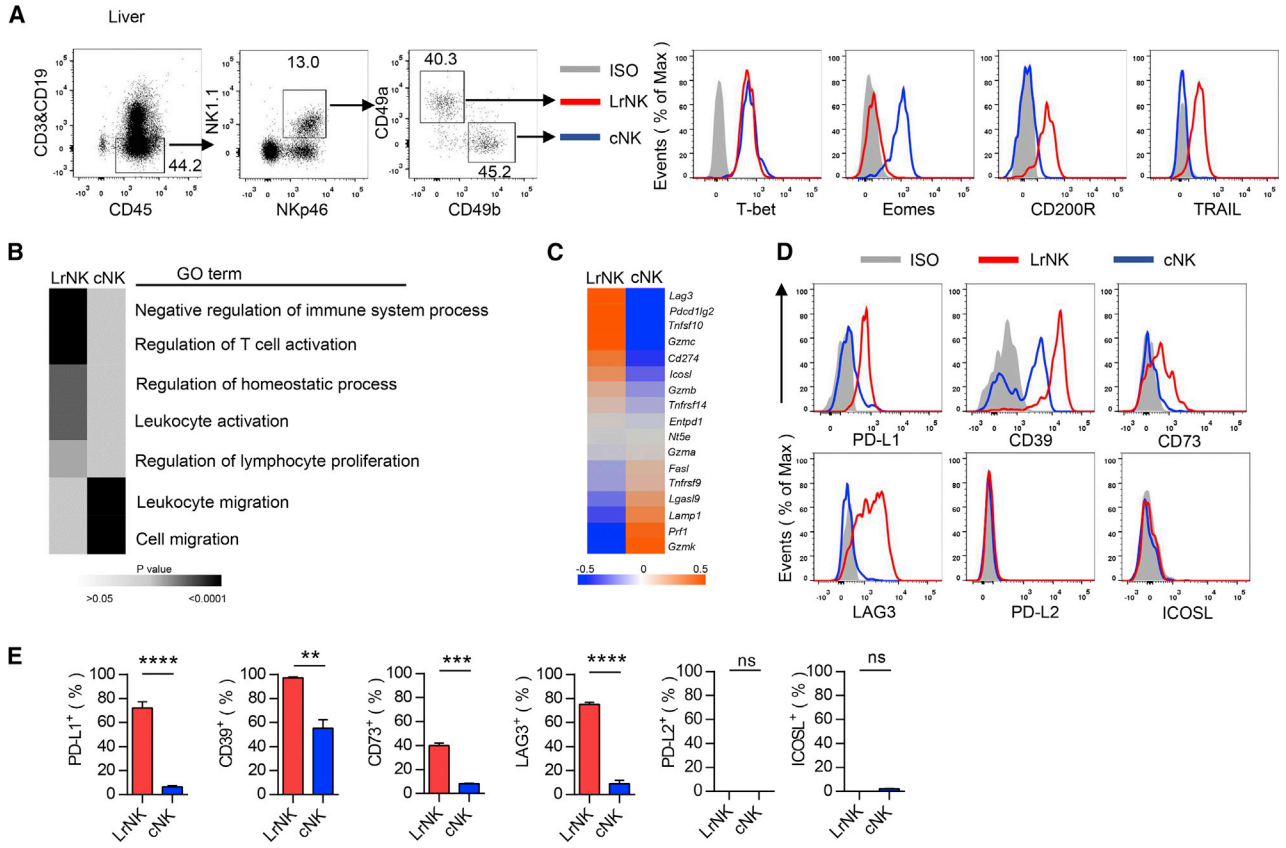

Figure 1. Negative Immune Regulators Are Enriched in Lrnk Cells

(A) Representative plots for the gating strategy of liver-resident NK (LrNK) cells ($CD45^+CD3^-CD19^-NK1.1^+NKp46^+CD49a^+CD49b^-$) and cNK cells ($CD45^+CD3^-CD19^-NK1.1^+NKp46^+CD49a^-CD49b^+$) from the livers of untreated normal WT B6 mice. Expression of T-bet, Eomes, CD200R, and TRAIL on the cells in the indicated populations is shown.

(B and C) Genome-wide transcriptional profiles of LrNK and liver cNK cells from a published dataset (GEO: GSE43339) (Peng et al., 2013). (B) Raw data were normalized by robust multiarray averaging (RMA, R package), and differences in gene expression were analyzed for screening for the genes with a fold change > 1.5 between LrNK and liver cNK cells. Gene Ontology (GO) term enrichment of the differentially expressed genes was analyzed with the Database for Annotation, Visualization, and Integrated Discovery (DAVID). GO terms with $p < 0.05$ related to immune responses are shown. (C) Heatmap of the expression of selected genes that are associated with immune regulation and cytotoxicity in LrNK and liver cNK cells.

(D) Flow-cytometry analysis of the indicated markers on LrNK and cNK cells in the livers of normal WT B6 mice.

(E) Statistical percentages of cells that express the indicated markers are shown.

Data represent at least three independent experiments with three to nine mice per group (mean ± SEM; ns, not significant; $^{**}p < 0.01$, $^{***}p < 0.001$, $^{****}p < 0.0001$).

Lohse, 2010). However, the precise cellular and molecular mechanisms underlying impaired T cell responses in hepatic tolerance induction are not fully understood.

Here, we found that LrNK cells negatively regulated the antiviral responses of hepatic T cells during acute and chronic viral infections and that this process was dependent on interaction between programmed death-1 (PD-1) and programmed death ligand 1 (PD-L1). In contrast, cNK cells promoted antiviral T cell responses. Our findings reveal distinct functions for LrNK cells and provide insight into the complex immune regulatory mechanisms that underlie local tolerance and immunity.

RESULTS

LrNK Cells Exhibit a Negative Regulatory Feature

In accordance with previous research (Tang et al., 2016; Weizman et al., 2017), $CD49a^+CD49b^-$ LrNK cells from wild-type (WT) mice at steady state highly expressed T-bet, CD200R, and tumor necrosis factor (TNF)-related apoptosis-inducing ligand (TRAIL) but lacked eomesodermin (Eomes) expression (Figure 1A). In contrast, $CD49a^-CD49b^+$ cNK cells were Eomes positive with nearly undetectable expression of CD200R and TRAIL (Figure 1A). To gain deeper insight into the functional roles of LrNK cells in immune responses, we compared the genome-wide transcriptional profiles of LrNK and liver cNK cells by using our previously published dataset (GEO: GSE43339) (Peng et al., 2013). Genes involved in negative regulation of the immune response were enriched in LrNK cells compared with cNK cells (Figure 1B). LrNK cells were characterized by high expression of negative regulatory genes encoding LAG3 (*Lag3*), programmed cell death 1 ligand 2 (PD-L2; *Pdcd1lg2*), TRAIL (*Tnfsf10*), PD-L1 (*Cd274*), and CD39 (*Entpd1*). In contrast, cNK cells preferentially expressed cytotoxic effect genes encoding granzyme

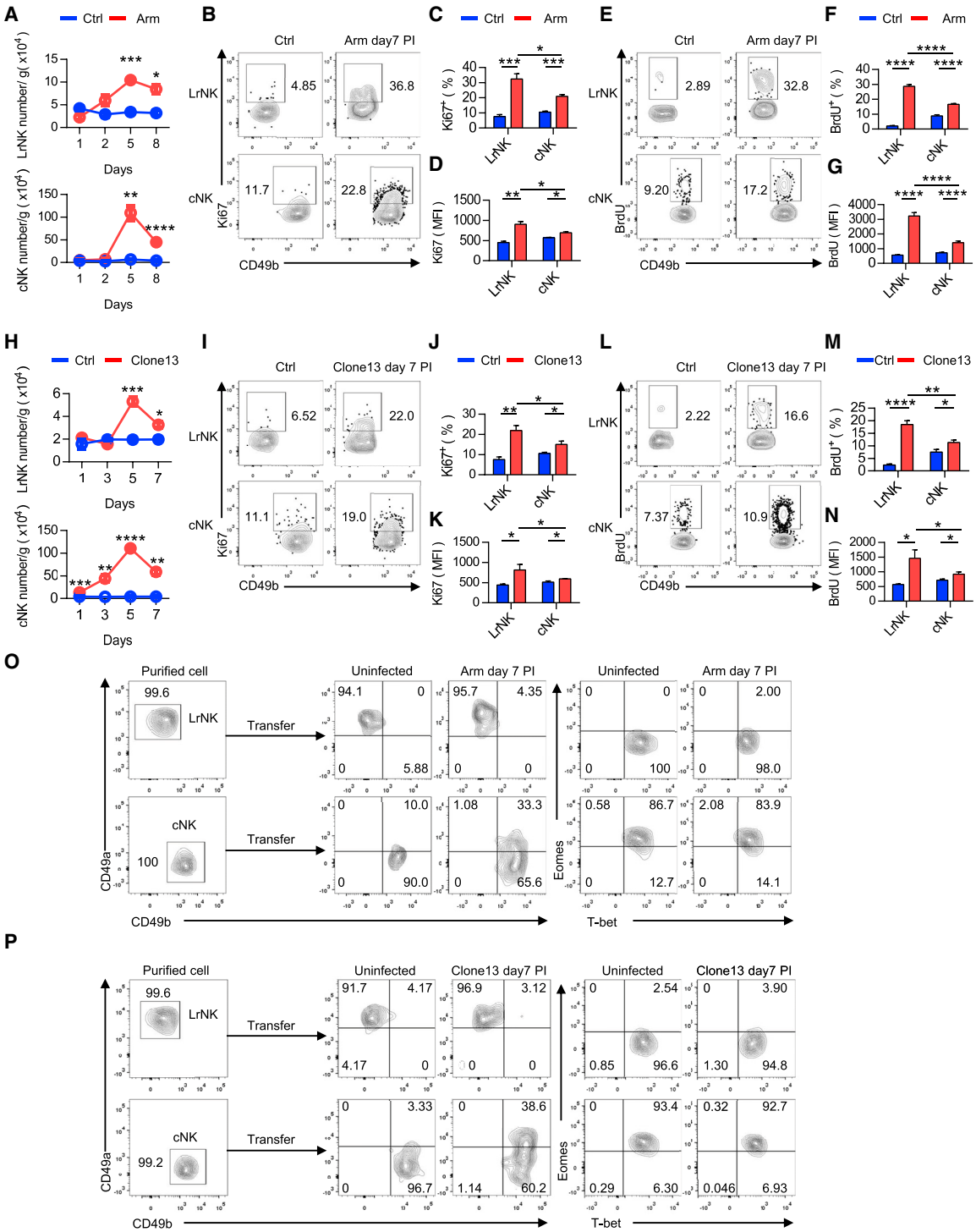

Figure 2. LrNK Cells Stably Maintain Their Identity and Proliferate Locally During Viral Infection

(A) Absolute numbers of LrNK and hepatic cNK cells in WT mice after LCMV Armstrong infection at the indicated time points.

(B) Representative plots show Ki67 staining of LrNK and cNK cells at LCMV Armstrong post-infection (PI) day 7.

(C and D) Percentages (C) and mean fluorescence intensity (MFI) (D) of the Ki67 expression in (B) are shown.

(E) Representative plots show BrdU incorporation in LrNK and cNK cells at LCMV Armstrong PI day 7.

(F and G) Percentages (F) and MFI (G) of the BrdU incorporation in (E) are shown.

(H) Absolute numbers of LrNK and hepatic cNK cells in WT mice after LCMV Clone13 infection at the indicated time points.

(I) Representative plots show Ki67 staining of LrNK and cNK cells at LCMV Clone13 PI day 7.

(J and K) Percentages (J) and MFI (K) of the Ki67 expression in (I) are shown.

(legend continued on next page)

A (*Gzma*), CD107a (*Lamp1*), perforin (*Prf1*), and granzyme K (*Gzmk*) (Figure 1C).

To confirm this trend, we used flow cytometry to assess the expression of molecules related to negative regulatory function on LrNK cells from WT mice at steady state. Consistent with the gene expression data, LrNK cells preferentially expressed TRAIL and PD-L1 (Figures 1A, 1D, and 1E), which can inhibit T cell responses via interaction with DR5 and PD-1 (Dong et al., 2004; Peppa et al., 2013; Schuster et al., 2014).

Moreover, compared with cNK cells, LrNK cells had higher expression of CD39, CD73, and LAG3 (Figures 1D and 1E), which are associated with immunosuppressive functions of regulatory T cells (Bauché et al., 2018; Deaglio et al., 2007; Huang et al., 2004). Although transcripts of PD-L2 and inducible co- stimulator (ICOS) ligand (ICOSL) were enriched in LrNK cells, flow-cytometry analysis showed undetectable surface expression (Figures 1C–1E). Collectively, these differences in genetic and molecular expression profiles between LrNK and cNK cells raise the possibility that LrNK cells are involved in suppressing adaptive immune responses.

LrNK Cells Might Proliferate Locally during Viral Infection

To explore whether LrNK cells are involved in shaping adaptive immunity, we used a mouse model of lymphocytic choriomeningitis virus (LCMV) infection, in which NK cells are unable to directly control LCMV replication (Bukowski et al., 1983; Welsh et al., 1991). Upon LCMV infection, NK cells accumulate dramatically in the liver (Liang et al., 2015; McIntyre and Welsh, 1986). However, the dynamic composition of NK cell subsets during this process is unknown. During acute (Armstrong) and chronic (Clone13) LCMV infection, we observed that the numbers of LrNK and cNK cells increased within the first week after infection and then gradually decreased (Figures 2A and 2H). To investigate whether the accumulation of NK cells in the liver was due to proliferation, we analyzed 5-bromo-2′-deoxyuridine (BrdU) incorporation and Ki67 staining by LrNK and cNK cells. At day 7 after LCMV infection, BrdU incorporation and Ki67 expression were increased in both NK cell subsets (Figures 2B–2G and 2I–2N). Moreover, LrNK cells proliferated more vigorously than cNK cells (Figures 2B–2G and 2I–2N). These results suggest that LrNK and cNK cells actively proliferate in response to viral infection.

LrNK cells represent a phenotypically stable lineage during homeostasis and MCMV infection (Peng et al., 2013; Tang et al., 2016; Weizman et al., 2017). To investigate whether they are able to maintain their phenotype during LCMV-induced inflammation, we sorted hepatic $CD49a^{+}CD49b^{-}$ LrNK cells and $CD49a^{-}CD49b^{+}$ cNK cells from CD45.1 mice and transferred them into sub-lethally irradiated WT CD45.2 mice, which were then infected with LCMV Armstrong or Clone13. The transferred LrNK cells migrated specifically to the recipient liver during infection (Figure S1), and they maintained a stable phenotype, as evidenced by the stable expression of CD49a and T-bet and lack of CD49b and Eomes (Figures 2O and 2P). In contrast, cNK cells exhibited increased CD49a expression after infection (Figures 2O and 2P), consistent with previous findings regarding the phenotypic plasticity of cNK cells in tumor- and MCMV-induced inflammatory microenvironments (Cortez et al., 2017; Gao et al., 2017; Weizman et al., 2017). However, despite the increased CD49a expression, cNK cells remained positive for CD49b and Eomes during infection, thus excluding the possibility that cNK cells are the source of the increase in LrNK cells during viral infection.

LrNK Cells Inhibit Hepatic T Cell Antiviral Responses during Acute Viral Infection

Considering the necessity of T-bet for LrNK cells' development, we crossed $Rag1^{-/-}$ mice with $Tbx21^{-/-}$ (T-bet-deficient) mice to obtain $Rag1^{-/-}Tbx21^{-/-}$ mice, which lacked LrNK cells and an adaptive immune system but had normal numbers of cNK cells in comparison with $Rag1^{-/-}Tbx21^{+/-}$ mice (Figures S2A–S2C). To provide more space for donor-derived T cells, we irradiated the $Rag1^{-/-}Tbx21^{-/-}$ mice and $Rag1^{-/-}Tbx21^{+/-}$ control mice before T cell transfer. Although irradiation led to a reduction in NK cells, cNK cells remained predominant in the livers of irradiated $Rag1^{-/-}Tbx21^{-/-}$ mice (Figures S2H–S2I). Furthermore, neither the phenotype nor the functions of LrNK and cNK cells were changed by irradiation, as evidenced by the stable expression of CD200R, TRAIL, CD49a, CD107a, granzyme B, IL-2, IFN-γ, TNF-α, and perforin (Figures S2H and S2J). After adoptive transfer of T cells into $Rag1^{-/-}Tbx21^{-/-}$ mice and $Rag1^{-/-}Tbx21^{+/-}$ control mice, the mice were infected with LCMV Armstrong and analyzed at day 7 after infection (Figure 3A). There were increased numbers of hepatic LCMV gp66-tetramer^{+} $CD4^{+}$ T cells and gp33-tetramer^{+} $CD8^{+}$ T cells, along with a reduced hepatic viral burden, in the $Rag1^{-/-}Tbx21^{-/-}$ mice compared with the control mice (Figures 3B and 3D–3F). In addition, the $Rag1^{-/-}Tbx21^{-/-}$ mice exhibited a higher serum alanine aminotransferase (ALT) concentration and increased lymphocyte infiltration in the liver (Figures 3C and 3G). These results imply that the absence of LrNK cells leads to enhanced antiviral T cell responses and exacerbated liver injury during LCMV Armstrong infection.

To further confirm the role of LrNK cells in acute LCMV infection, we adoptively transferred $CD49a^{+}CD49b^{-}$ LrNK cells and $CD49a^{-}CD49b^{+}$ cNK cells from CD45.1 mice into sub-lethally irradiated WT CD45.2 mice, which were then infected with LCMV Armstrong (Figure 3H). After 7 days of infection, the transfer of LrNK cells led to decreased numbers of hepatic LCMV gp66-tetramer^{+} $CD4^{+}$ T cells and gp33-tetramer^{+} $CD8^{+}$ T cells, an increased hepatic viral burden, and a reduced serum ALT concentration (Figures 3I–3M). In contrast, the transfer of cNK cells had the opposite effects (Figures 3I–3M).

(L) Representative plots show BrdU incorporation of LrNK and cNK cells at LCMV Clone13 PI day 7.
(M and N) Percentages (M) and MFI (N) of the BrdU incorporation in (L) are shown.
(O and P) 2×10^{5} LrNK or cNK cells were sorted from the livers of CD45.1^{+} WT mice and adoptively transferred intravenously into sub-lethally irradiated CD45.2^{+} congenic recipient mice. Mice were subsequently infected with LCMV Armstrong (O) or Clone13 (P). Representative plots show CD49a, CD49b, T-bet, and Eomes staining of donor cells before transfer and after recovery from recipient livers at PI day 7.
Data represent three independent experiments with three to ten mice per group (mean ± SEM; *$p < 0.05$, **$p < 0.01$, ***$p < 0.001$, ****$p < 0.0001$).

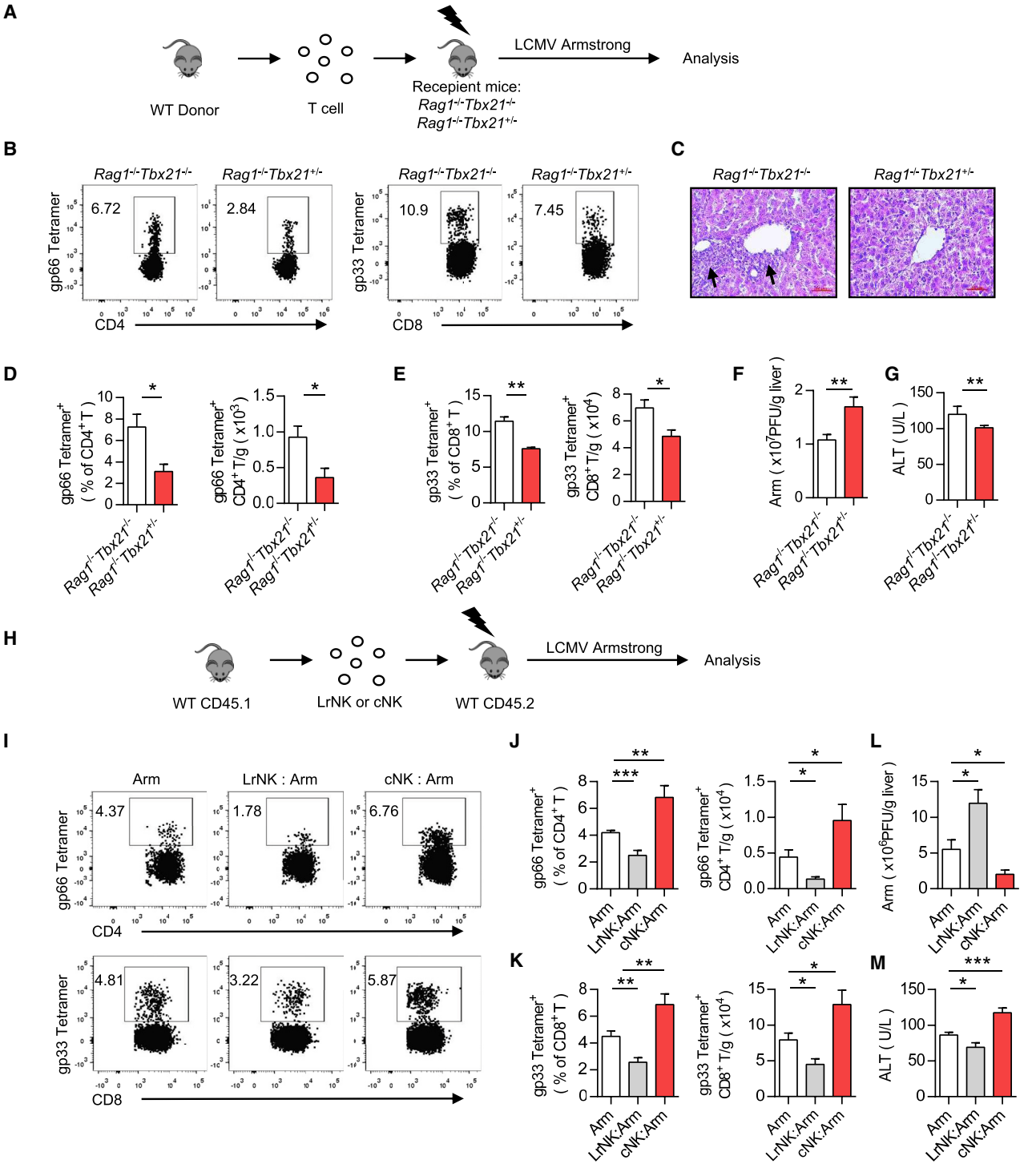

Figure 3. LrNK Cells Inhibit Hepatic T Cell Responses against LCMV Armstrong Infection

(A) 1 × 10^6 T cells from WT mice were sorted and transferred into sub-lethally irradiated *Rag1*$^{-/-}$*Tbx21*$^{-/-}$ and *Rag1*$^{-/-}$*Tbx21*$^{+/-}$ mice. Recipient mice were then infected with LCMV Armstrong and analyzed at PI day 7.

(B) Representative plots show gp66-specific CD4$^+$ T cells and gp33-specific CD8$^+$ T cells from livers of the recipient mice in (A).

(C) Representative hematoxylin and eosin (H&E) staining images of the liver samples in (A) are shown, and the black arrows indicate lymphocyte infiltration. Scale bars represent 50 μm.

(D and E) Ratio (D) and absolute numbers (E) of the gp66-specific CD4$^+$ T cells and gp33-specific CD8$^+$ T cells in (B) are shown.

(F) Viral titers in the livers from the recipient mice in (A) were analyzed at PI day 7.

(legend continued on next page)

Thus, these data indicate that LrNK cells can inhibit antiviral T cell responses.

We then analyzed T cell responses in other organs of mice that received T cells and were infected with LCMV Armstrong (Figure 3A), and we found no difference in the number of antigen-specific T cells or viral titers in the spleens and lungs between *Rag1*$^{-/-}$*Tbx21*$^{-/-}$ and control recipients (Figures S3D–S3G). Altogether, with the lack of changes in splenic T cell responses and viral titers after LrNK cell transfer (Figures 3H and S3A–S3C), these results suggest that LrNK-cell-mediated inhibition of antiviral T cell responses is restricted to the liver without affecting other organs.

To explore whether the above conclusions also apply to other virus-induced acute infections, we then utilized a mouse model of acute adenovirus infection, in which bulk NK cells promote T cell responses (Liu et al., 2000) but in which LrNK cell function has not previously been studied. After adoptive transfer of T cells into *Rag1*$^{-/-}$*Tbx21*$^{-/-}$ mice that were then infected with adenovirus, more CD4^{+} and CD8^{+} T cells were present in the livers of the *Rag1*$^{-/-}$*Tbx21*$^{-/-}$ mice, which also showed higher IFN-γ and TNF-α expression, than in the livers of control mice at day 7 after infection (Figures S4A–S4D). Consistent with this finding, *Rag1*$^{-/-}$*Tbx21*$^{-/-}$ mice exhibited a lower viral load in the liver and a higher ALT concentration than the control mice (Figures S4E and S4F). Notably, this process was reversed by adoptive transfer of T cells along with LrNK cells into the *Rag1*$^{-/-}$*Tbx21*$^{-/-}$ mice (Figures S4A–S4F). Furthermore, in line with the observations during LCMV Armstrong infection, adoptive transfer of LrNK cells into WT mice, which were then infected with adenovirus, also inhibited T cell antiviral immunity, decreased lymphocyte infiltration, increased the viral burden in the liver, and reduced the serum ALT concentration, whereas cNK cells caused the reverse phenomena (Figures S4G–S4M).

In accordance with previous reports showing that T-bet regulates the terminal maturation of cNK cells (Gordon et al., 2012; Soderquest et al., 2011; Townsend et al., 2004), we also found that there was a dramatic reduction in the most mature CD11b^{+-}CD27^{-} cNK cells in the *Rag1*$^{-/-}$*Tbx21*$^{-/-}$ mice (Figure S2A). To assess whether the lack of CD11b^{+}CD27^{-} cNK cells contributed to the enhanced T cell responses in *Rag1*$^{-/-}$*Tbx21*$^{-/-}$ mice, we adoptively transferred T cells along with CD11b^{+}CD27^{-} cNK cells into *Rag1*$^{-/-}$*Tbx21*$^{-/-}$ mice. However, these recipients displayed more robust T cell responses after infection than the control mice (Figures S4A–S4F), suggesting that the enhanced antiviral T cell responses in *Rag1*$^{-/-}$*Tbx21*$^{-/-}$ mice resulted from the lack of LrNK cells rather than the lack of terminally mature cNK cells. Collectively, the above observations indicate that LrNK cells effectively restrain T cell responses during acute viral infection, whereas cNK cells have the opposite effect.

LrNK Cells Inhibit Hepatic T Cell Antiviral Responses during Chronic Viral Infection

To investigate whether LrNK cells exert similar roles during chronic viral infection, we used a murine model of chronic infection involving LCMV Clone13 (Lang et al., 2012; Waggoner et al., 2011). Similar to the findings observed in acute viral infections, compared with control mice, *Rag1*$^{-/-}$*Tbx21*$^{-/-}$ mice that received an adoptive T cell transfer and underwent infection with LCMV Clone13 exhibited a higher number of antigen-specific T cells and enhanced cytokine secretion by T cells in the liver (Figures 4A–4F). Additionally, a lower viral titer, increased lymphocyte infiltration in the liver, and a higher serum ALT concentration were also detected in *Rag1*$^{-/-}$*Tbx21*$^{-/-}$ mice (Figures 4G–4I), suggesting that LrNK cells restrain T cell responses during chronic viral infection.

To further verify the negative regulatory role of LrNK cells during chronic viral infection, we evaluated T cell function in WT mice that received an LrNK or a cNK cell transfer followed by challenge with LCMV Clone13 (Figure 4J). LrNK cells effectively reduced the number of antigen-specific T cells, leading to a higher viral burden in the liver and a lower serum ALT concentration, whereas cNK cells still played an opposing role (Figures 4K–4P). We then used *Ncr1*(NKp46)$^{Cre/+}$*Eomes*$^{fl/fl}$ mice, in which cNK cells are specifically reduced but LrNK cells are not affected (Weizman et al., 2017). After LCMV Clone13 infection for 14 days, these mice exhibited fewer virus-specific T cells, a lower serum ALT concentration, and higher viral titers in the liver and spleen than littermate *Ncr1*$^{+/+}$*Eomes*$^{fl/fl}$ control mice (Figures 4Q–4T), further suggesting that LrNK cells rather than cNK cells mediate inhibition of virus-specific T cell responses. Thus, these results show that LrNK cells can negatively regulate antiviral T cell responses and thereby impair viral clearance during chronic viral infection.

LrNK Cells Increase PD-L1 Expression during Acute and Chronic Viral Infection

Despite the absence of LrNK cells in *Rag1*$^{-/-}$*Tbx21*$^{-/-}$ mice, there were no differences regarding cytokine secretion or cytotoxic molecule release by the total NK cell population between *Rag1*$^{-/-}$*Tbx21*$^{-/-}$ and control mice upon virus challenge (Figures S2D–S2G). This suggests that LrNK cells do not inhibit T cells' responses via cytokines or direct cytotoxicity. To investigate potential mechanisms by which LrNK cells regulate virus-specific T cell responses, we analyzed surface expression of immunosuppressive molecules on LrNK cells during viral infections. Flow-cytometry analysis revealed increased PD-L1 expression on LrNK cells at day 7 after LCMV and adenovirus infection, whereas TRAIL expression was remarkably decreased on LrNK cells after viral infection (Figures 5A, 5B, 5E, 5F, 5I, and 5J). Furthermore, high expression of PD-1, the receptor for

(G) Serum ALT concentrations from recipient mice in (A) are shown.
(H) 2 × 10^{5} LrNK and cNK cells from CD45.1^{+} mice were sorted and adoptively transferred into sub-lethally irradiated CD45.2^{+} mice, and the recipient mice were then infected with LCMV Armstrong and analyzed at PI day 7.
(I) Representative plots show gp66-specific CD4^{+} T cells and gp33-specific CD8^{+} T cells from livers of the recipient mice in (H).
(J and K) Ratio (J) and absolute numbers (K) of hepatic gp66-specific CD4^{+} T cells and gp33-specific CD8^{+} T cells from the recipient mice in (I) are shown.
(L and M) Viral titers in the livers (L) and serum ALT concentrations (M) were measured at PI day 7.
Data represent three or four independent experiments with four to eight mice per group (mean ± SEM; *p < 0.05, **p < 0.01, ***p < 0.001).
See also Figures S1–S4.

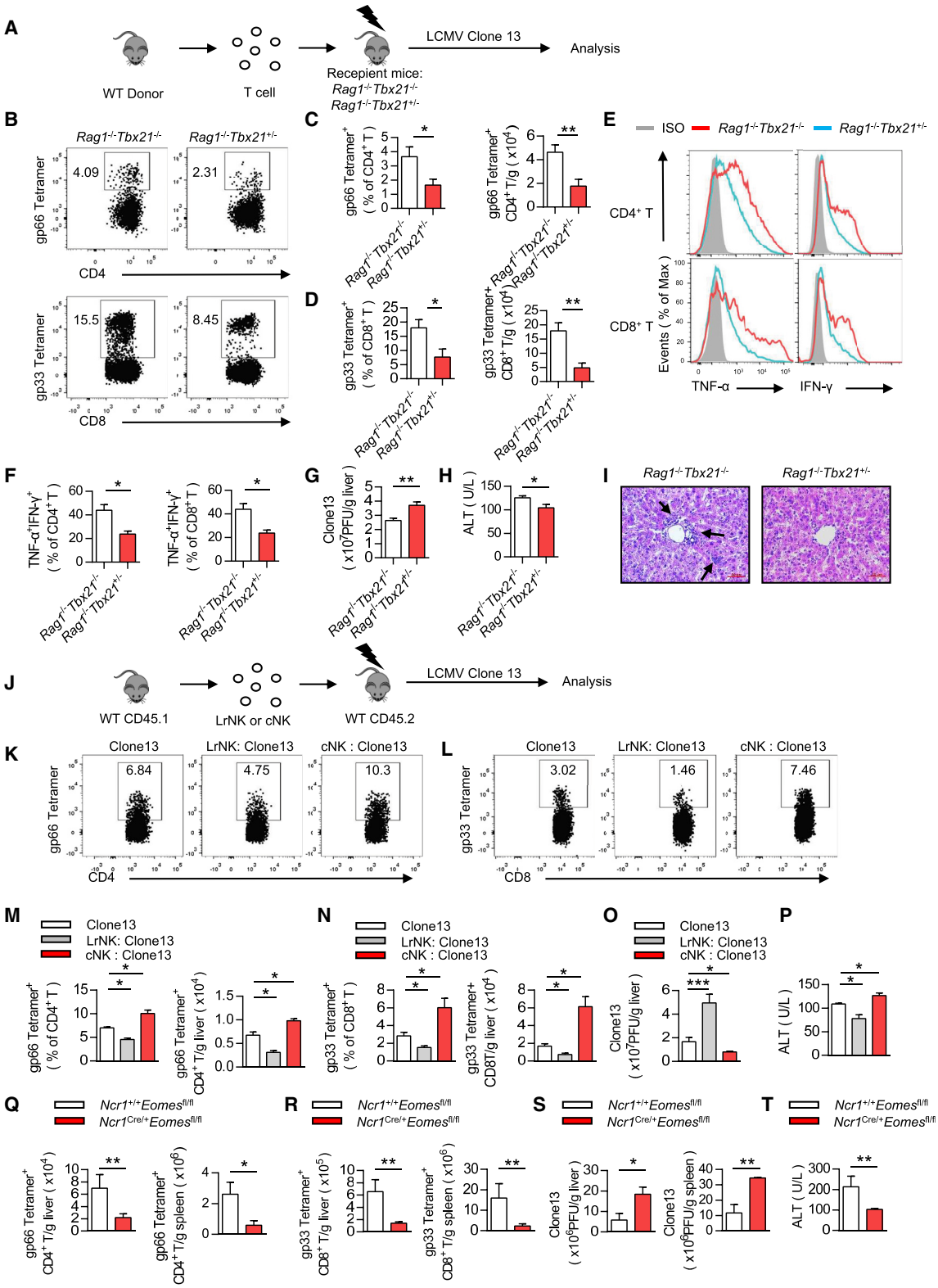

Figure 4. LrNK Cells Inhibit Hepatic T Cell Responses against Chronic LCMV Clone13 Infection

(A) 1 × 10^6 T cells from WT mice were sorted and transferred into sub-lethally irradiated *Rag1*$^{-/-}$*Tbx21*$^{-/-}$ and *Rag1*$^{-/-}$*Tbx21*$^{+/-}$ mice. Recipient mice were then infected with LCMV Clone13 and analyzed at PI day 14.

(B) Representative plots show gp66-specific CD4$^+$ T cells and gp33-specific CD8$^+$ T cells from the livers of the recipient mice in (A).

(legend continued on next page)

PD-L1, was observed on hepatic $CD4^+$ and $CD8^+$ T cells after viral infection, whereas DR5, the receptor for TRAIL, was not expressed by hepatic T cells (Figures 5C, 5D, 5G, 5H, 5K, and 5L). We also examined the expression of two other immunosuppressive molecules, CD39 and CD73, which are important for Treg cell functionality, involving the conversion of ATP to adenosine (Deaglio et al., 2007; Gu et al., 2017). LrNK cells maintained high expression of CD39 but decreased CD73 expression after LCMV Armstrong infection (Figure S5), suggesting that CD39 and CD73 might not be involved in LrNK-cell-mediated regulation of T cells. Thus, these findings raise the possibility that LrNK cells interact with T cells via PD-L1-PD-1 to exert suppressive functions.

LrNK Cells Regulate T Cell Functions via PD-L1 Checkpoint Control

To explore whether PD-L1 is responsible for LrNK-cell-mediated suppression of antiviral T cell responses, we pre-incubated LrNK cells with neutralizing anti-PD-L1 antibodies (Abs) before adoptive transfer into LCMV-Armstrong- or Clone13-infected mice (Figures 6A and S7A). *Ex vivo* blockade of PD-L1 on LrNK cells prior to adoptive transfer did not affect the *in vivo* trafficking of LrNK cells after virus challenge (Figure S6). After PD-L1 blockade, the number and proliferation of hepatic virus-specific T cells were higher than and the cytokine-producing abilities of the hepatic T cells were superior to those in the mice receiving LrNK cells without PD-L1 blockade (Figures 6B–6G, 6J–6N, and S7B–S7M), implying that PD-L1 expression on LrNK cells negatively regulates hepatic T cell responses. Moreover, blockade of PD-L1 on LrNK cells led to an increased serum ALT concentration (Figures 6I and S7O) and a decreased viral load (Figures 6H and S7N). To confirm the role of the PD-1-PD-L1 axis in LrNK-cell-mediated regulation, we transferred T cells from *Pdcd1*$^{-/-}$ (PD-1-deficient) mice into *Rag1*$^{-/-}$*Tbx21*$^{-/-}$ and *Rag1*$^{-/-}$*Tbx21*$^{+/-}$ control mice, which were analyzed 14 days after LCMV Clone13 infection (Figure S7P). We found no differences regarding the number of hepatic antigen-specific T cells, viral titer, or ALT concentration between *Rag1*$^{-/-}$*Tbx21*$^{-/-}$ and control mice (Figures S7Q–S7V). Combined with the earlier finding that WT-derived T cells exhibited more robust antiviral responses in *Rag1*$^{-/-}$*Tbx21*$^{-/-}$ mice than in control mice (Figures 4A–4H), these data confirm that LrNK cells control the antiviral activity of hepatic T cells via the PD-1-PD-L1 axis.

To further investigate whether LrNK cells directly inhibit T cell responses, we co-cultured T cells with NK cell subsets in the presence of anti-CD3 and -CD28 monoclonal Abs. Co-culture with LrNK cells suppressed the proliferation of both $CD4^+$ and $CD8^+$ T cells, whereas the presence of cNK cells augmented T cell proliferation (Figures 7A and 7B). Furthermore, the inhibitory role of LrNK cells was mediated by cell-cell contact and not by soluble factors, as evidenced by Transwell assays (Figures 7C and 7D). This indicates that LrNK cells directly regulate T cell responses. Additionally, blockade of PD-L1 in the co-culture system restored T cell proliferation in the presence of LrNK cells, whereas blockade of TRAIL did not (Figure 7E). Therefore, these data collectively demonstrate that LrNK cells directly suppress T cell responses via the engagement of the PD-L1 checkpoint.

DISCUSSION

NK cells are crucial effectors of innate immunity and also act as modulators of adaptive immune responses (Crome et al., 2013; Schuster et al., 2016; Waggoner et al., 2011). However, previous studies focused on bulk NK cells, which are now known to be a mixture of cNK cells, tissue-resident NK cells, and mucosal ILC1s (Artis and Spits, 2015). The respective roles of different NK cell subsets in regulating adaptive immune responses are unclear. In this study, we investigated the contribution of liver NK cell subsets to adaptive immunity in the context of viral infections and defined distinct functions of LrNK and cNK cells.

The liver is an attractive target site for pathogens because of its immune tolerogenic properties (Gao, 2016; Li and Tian, 2013; Protzer et al., 2012). The liver contains a high frequency of NK cells in comparison with other tissues, and LrNK cells account for nearly half of the hepatic bulk NK cells (Peng et al., 2013). Expression of the inhibitory receptor NKG2A on NK cells contributes to HBV persistence (Li et al., 2013). LrNK cells preferentially express NKG2A in comparison with cNK cells, and the absence of NKG2A results in enhanced activation of DCs and expansion of virus-specific $CD8^+$ T cells during adenovirus infection (Krueger et al., 2017). Whether this effect is mediated by LrNK cells directly is unclear. By using *Rag1*$^{-/-}$*Tbx21*$^{-/-}$ mice lacking both LrNK cells and T cells, we found that transferred T cells in these mice exhibited enhanced antiviral activity, which we reversed by adding back LrNK cells. In addition to seeing a loss of LrNK cells in *Rag1*$^{-/-}$*Tbx21*$^{-/-}$ mice, we also observed a reduction in terminally mature $CD11b^+CD27^-$ cNK cells, consistent with previous observations in *Tbx21*$^{-/-}$ mice (Sodersquest et al., 2011; Townsend et al., 2004). However, adding back

(C and D) Ratio (C) and absolute numbers (D) of the gp66-specific $CD4^+$ T cells and gp33-specific $CD8^+$ T cells in (B) are shown.
(E) Expression of TNF-α and IFN-γ by $CD4^+$ and $CD8^+$ T cells of the recipient mice in (A).
(F) Quantification of intracellular TNF-α and IFN-γ staining of the $CD4^+$ and $CD8^+$ T cells in (E).
(G and H) Viral titers in the livers (G) and serum ALT concentrations (H) were measured at PI day 14.
(I) Representative H&E staining images of the liver samples in (A) are shown, and the black arrows indicate lymphocyte infiltration. Scale bars represent 50 μm.
(J) 2×10^5 LrNK and cNK cells from $CD45.1^+$ mice were adoptively transferred into sub-lethally irradiated $CD45.2^+$ mice, and the recipient mice were then infected with LCMV Clone13 and analyzed at PI day 14.
(K and L) Representative plots show hepatic gp66-specific $CD4^+$ T cells (K) and gp33-specific $CD8^+$ T cells (L) of the recipient mice in (J).
(M and N) Ratio (M) and absolute numbers (N) of gp66-specific $CD4^+$ T cells and gp33-specific $CD8^+$ T cells in (K and L) are shown.
(O and P) Viral titers in the livers (O) and serum ALT concentrations (P) were measured at PI day 14.
(Q–T) *Ncr1*$^{Cre/+}$*Eomes*$^{fl/fl}$ mice and littermate *Ncr1*$^{+/+}$*Eomes*$^{fl/fl}$ control mice were infected with LCMV Clone13 and analyzed at PI day 14. The absolute numbers of gp66-specific $CD4^+$ T cells (Q) and gp33-specific $CD8^+$ T cells (R) in the livers and spleens are shown. Viral titers (S) and serum ALT concentrations (T) were measured at PI day 14.
Data represent two independent experiments with three to six mice per group (mean ± SEM; *$p < 0.05$, **$p < 0.01$, ***$p < 0.001$).

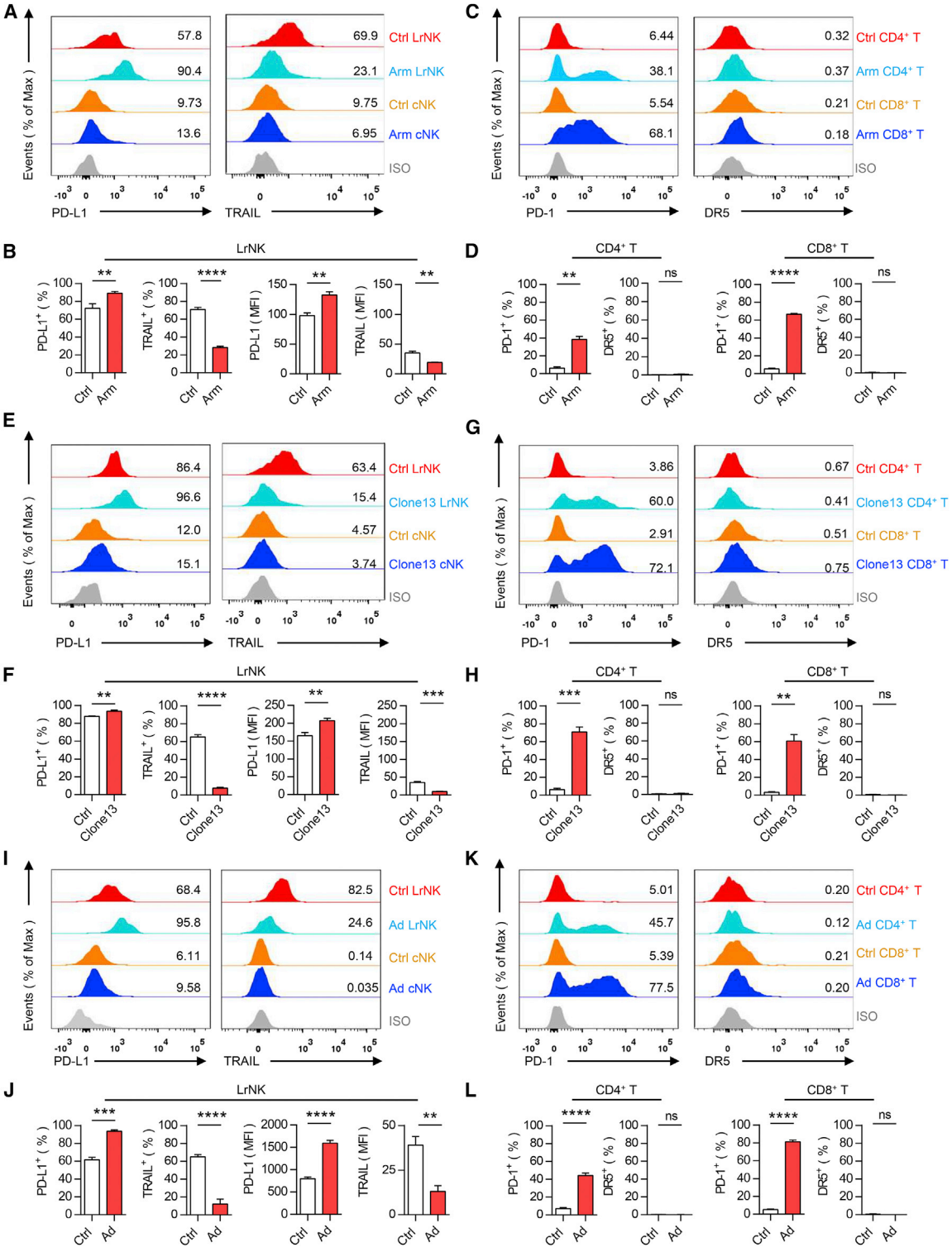

Figure 5. LrNK Cells Increase PD-L1 Expression During Viral Infection

(A) Representative histograms show the expression of PD-L1 and TRAIL on LrNK and cNK cells from LCMV-Armstrong-infected WT mice at PI day 7.

(B) Percentages and MFI of the PD-L1 and TRAIL expression on LrNK cells in (A) are shown.

(C) Representative histograms show the expression of PD-1 and DR5 on hepatic $CD4^+$ and $CD8^+$ T cells from LCMV-Armstrong-infected WT mice at PI day 7.

(D) Percentages of the PD-1 and DR5 expression on hepatic $CD4^+$ and $CD8^+$ T cells in (C) are shown.

(E) Representative histograms show the expression of PD-L1 and TRAIL on LrNK and cNK cells from LCMV-Clone13-infected WT mice at PI day 7.

(F) Percentages and MFI of the PD-L1 and TRAIL expression on LrNK cells in (E) are shown.

(legend continued on next page)

terminally mature cNK cells to *Rag1*$^{-/-}$*Tbx21*$^{-/-}$ mice further promoted antiviral T cell responses, suggesting that the enhanced T cell functions in *Rag1*$^{-/-}$*Tbx21*$^{-/-}$ mice were due to the loss of LrNK cells and not the loss of terminally mature cNK cells. By performing adoptive-cell-transfer experiments using LrNK-cell-deficient mice, we demonstrated that LrNK cells inhibited the antiviral responses of hepatic T cells and thus led to slower viral clearance and reduced liver inflammation. The immunosuppressive function of LrNK cells provides insight into the cellular basis of liver tolerance.

There is accumulating evidence of bulk NK-cell-mediated impairment of virus-specific T cell immunity in LCMV infection models (Lang et al., 2012; Waggoner et al., 2011; Waggoner et al., 2010). In contrast, during acute adenovirus infection, NK cells release IFN-γ to facilitate antiviral T cells responses (Krueger et al., 2017; Liu et al., 2000). Possible explanations for this disparity in NK cell function include differences between studies in the viral species or dose, timing of NK cell depletion, and mouse strain. Virus-specific CD8$^+$ T cells display enhanced IFN-γ production in *Nfil3*$^{-/-}$ mice after infection with the strain LCMV WE (Lang et al., 2012). However, in addition to the loss of cNK cells, the number of LrNK cells, ILC2s, and ILC3s are simultaneously reduced in *Nfil3*$^{-/-}$ mice (Geiger et al., 2014; Seillet et al., 2014; Tang et al., 2016). ILC2s and ILC3s are also able to regulate T cell responses (Hepworth et al., 2013; Schwartz et al., 2017). Therefore, whether the enhanced T cell responses in *Nfil3*$^{-/-}$ mice are caused by a lack of cNK cells or a lack of other cell types is unclear from this previous study (Lang et al., 2012). By using *Ncr1*$^{Cre/+}$*Eomes*$^{fl/fl}$ mice that are specifically deficient in cNK cells, we found lower virus-specific T cell responses in these mice compared with littermate *Ncr1*$^{+/+}$*Eomes*$^{fl/fl}$ control mice, suggesting a role for cNK cells in the promotion of T cell responses during viral infection. Although the mechanism was not explored deeply in our study, previous research suggests that NK cells can be recruited to lymph nodes, where they secrete IFN-γ to induce Th1 responses (Martín-Fontecha et al., 2004). Considering the strong migratory capacity of cNK cells, this might provide an explanation for the enhanced antiviral T cell responses induced by cNK cells.

PD-1 blockade can lead to improved immune responses to LCMV infection (Ahn et al., 2018; Barber et al., 2006; Mueller et al., 2010; Penaloza-MacMaster et al., 2014). The PD-1-PD-L1 pathway curbs inflammation in the liver (Dong et al., 2004) and inhibits antiviral immunity during adenovirus infection (Iwai et al., 2003). However, the cellular pathways involved in these processes have not been clearly demonstrated. Here, we found that LrNK cells had high expressions of immunosuppressive molecules at steady state. In particular, the immune checkpoint inhibitor PD-L1 was constitutively expressed on LrNK cells and further increased during viral infections, and its receptor PD-1 was concurrently increased on T cells. Consistent with previous evidence showing impaired T cell responses induced by the PD-1-PD-L1 axis (Dong et al., 2004; Schildberg et al., 2016), treatment of LrNK cells with Abs blocking PD-L1 effectively restored antiviral T cell functions *in vivo* and enhanced T cell proliferation *in vitro*. These findings suggest that LrNK cells negatively regulate T cell responses via a PD-L1-dependent mechanism.

In chronic MCMV infection, CD4$^+$ T cells accumulate in the salivary glands and show elevated expression of the TRAIL receptor, rendering them vulnerable to TRAIL-mediated lysis (Schuster et al., 2014). This lysis process is thought to be mediated by TRAIL expressed on salivary gland NK cells. In addition, in human chronic HBV infection, NK cells negatively regulate antiviral T cell responses in a TRAIL-dependent manner (Peppa et al., 2013). Notably, LrNK cells also expressed high amounts of TRAIL at steady state. However, after infection with LCMV or adenovirus for 7 days, TRAIL expression on LrNK cells was decreased, and the expression of its receptor DR5 on hepatic T cells remained low. These findings are further supported by the observation that blocking TRAIL had no effect on T cell proliferation during co-culture of T and LrNK cells, suggesting that TRAIL is dispensable for LrNK-cell-mediated T cell suppression.

Human NK cells are also thought to have a negative regulatory function. CD56^{bright}CD27$^+$ decidual NK cells function as key regulatory cells to maintain maternal-fetal tolerance by secreting IFN-γ to dampen Th17 cells (Fu et al., 2013). CD56$^+$CD3$^-$ cells in tumor-infiltrating lymphocyte cultures can suppress T cell expansion via NKp46 (Crome et al., 2017). Unique NK cell subsets resembling murine LrNK cells are also present in humans. Human CXCR6$^+$ or CD49e$^-$ NK cells, which are specifically enriched in the liver but rare in the circulation, are considered human LrNK cells (Aw Yeang et al., 2017; Cuff et al., 2016; Stegmann et al., 2016). However, these LrNK cells selectively express Eomes rather than T-bet (Aw Yeang et al., 2017; Harmon et al., 2016), in contrast to T-bet$^+$Eomes$^-$ mouse LrNK cells (Sojka et al., 2014). The functional differences of cytokine production and degranulation capacity between human LrNK cells and cNK cells are still controversial (Aw Yeang et al., 2017; Harmon et al., 2016), and the primary physiological function of human LrNK cells remains to be fully determined. PD-1 blockade can enhance HBV-specific CD8$^+$ T cell proliferation and inflammatory cytokine production (Zhang et al., 2008), suggesting that a negative signaling pathway is in operation in human HBV infection. PD-1 is also implicated in impairment of virus-specific T cells from HCV-infected patients (Raziorrouh et al., 2011; Urbani et al., 2008). Thus, together with our findings regarding murine LrNK cells, these results show that it will be of interest to investigate whether human LrNK cells can also negatively regulate T cell responses via the PD-1-PD-L1 axis during hepatotropic virus infection.

(G) Representative histograms show the expression of PD-1 and DR5 on hepatic CD4$^+$ and CD8$^+$ T cells from LCMV-Clone13-infected WT mice at PI day 7.
(H) Statistical percentages of cells that express the indicated markers in (G) are shown.
(I) Representative histograms show the expression of PD-L1 and TRAIL on LrNK and cNK cells from adenovirus-infected WT mice at PI day 7.
(J) Percentages and MFI of the PD-L1 and TRAIL expression on LrNK cells in (I) are shown.
(K) Representative histograms show the expression of PD-1 and DR5 on hepatic CD4$^+$ and CD8$^+$ T cells from adenovirus-infected WT mice at PI day 7.
(L) Statistical percentages of cells that express the indicated markers in (K) are shown.
Data represent three to five independent experiments with three to five mice per group (mean ± SEM; ns, not significant; $^{**}p < 0.01$, $^{***}p < 0.001$, $^{****}p < 0.0001$). See also Figure S5.

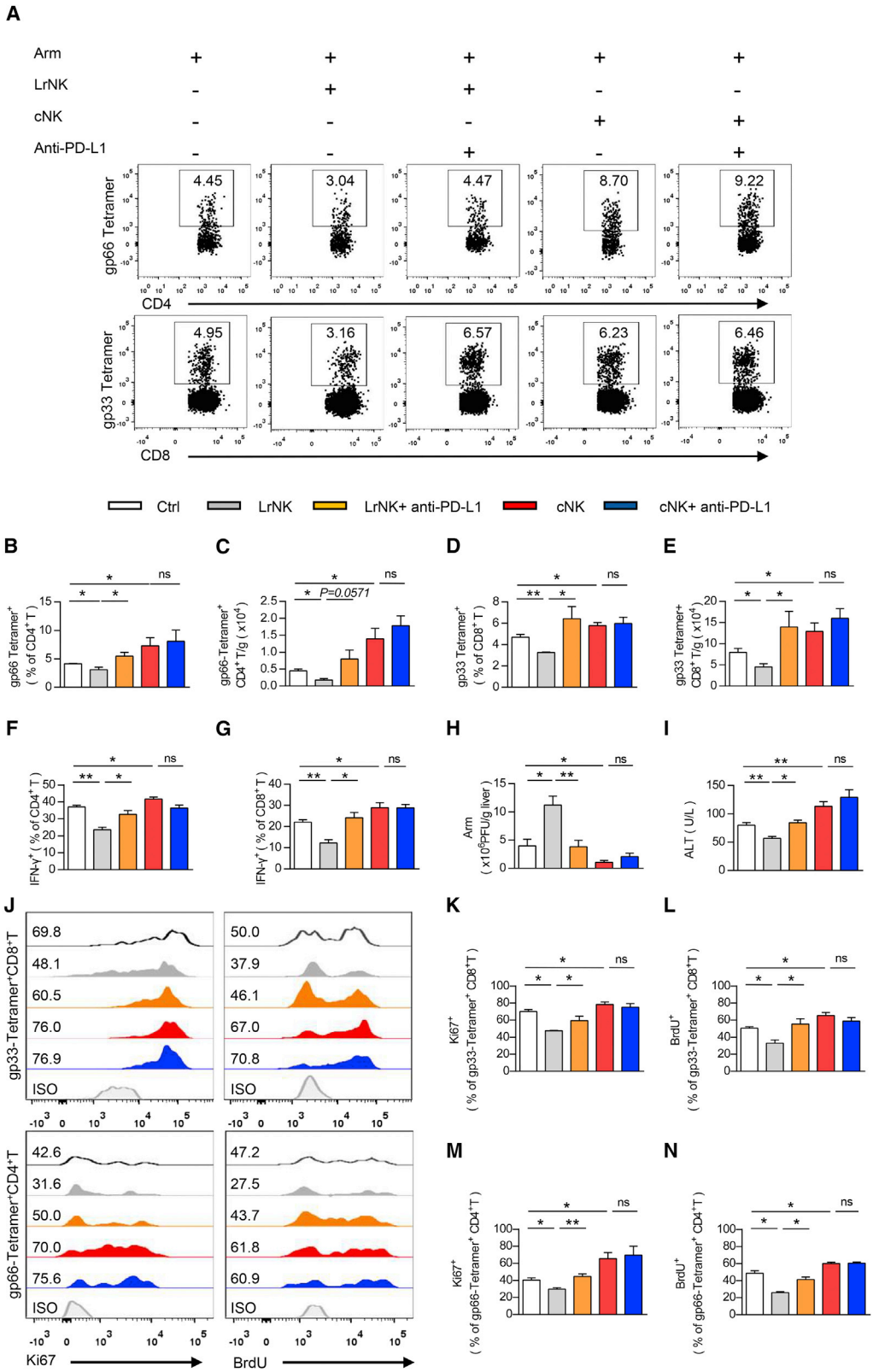

(legend on next page)

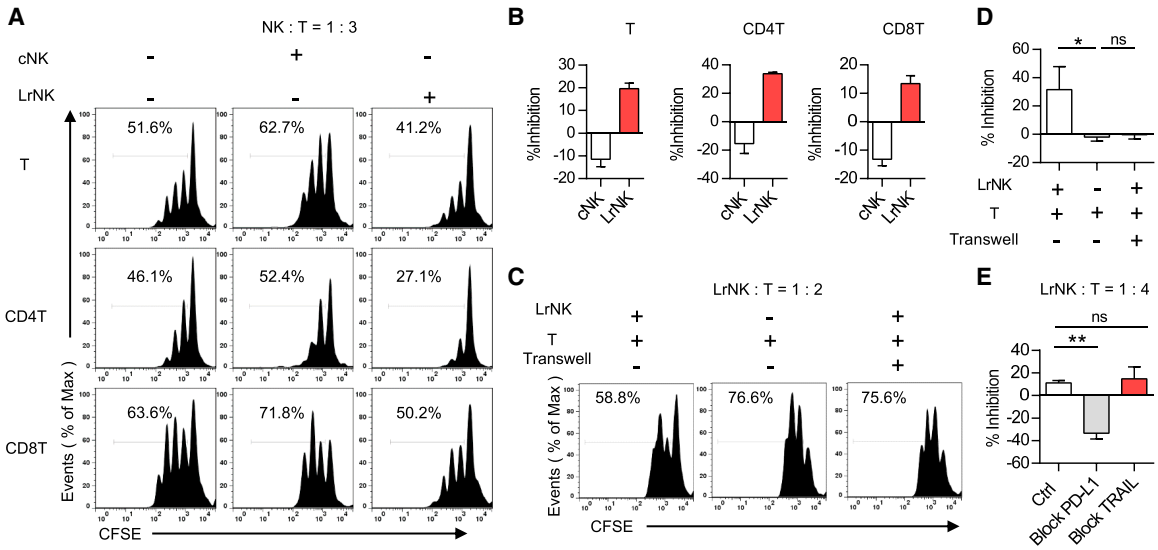

Figure 7. LrNK Cells Directly Inhibit T Cell Proliferation *In Vitro*

(A) Purified T cells from the livers of WT mice were labeled with carboxyfluorescein diacetate succinimidyl ester (CFSE) and cultured for 3 days in the presence of anti-CD3 and -CD28 mAb with or without purified LrNK and cNK cells at a 3:1 ratio of T cells to NK cells. $CD4^+$ and $CD8^+$ T cells were analyzed by CFSE dilution.

(B) Statistical results from the cells in (A) are shown.

(C) LrNK cells were co-cultured with CFSE-labeled T cells or cultured separately (with a Transwell system) for 3 days at a 1:2 ratio of LrNK cells to T cells in the presence of anti-CD3 and -CD28 mAb. T cells were analyzed by CFSE dilution.

(D) Statistical results from the cells in (C) are shown.

(E) LrNK cells were co-cultured with CFSE-labeled T cells for 3 days at a 1:4 ratio of LrNK cells to T cells in the presence of neutralizing mAbs against mouse PD-L1 or TRAIL. T cells were analyzed by CFSE dilution. Statistical results are shown.

Data are representative from represent two to four independent experiments (mean ± SEM; ns, not significant; *$p < 0.05$, **$p < 0.01$).

However, because the immune microenvironment is complex, it still cannot be concluded that LrNK cells inhibit T cells in all settings. In different circumstances, NK cells might perform distinct roles. Given that LrNK cells can efficiently produce multiple cytokines, such as IFN-γ, TNF-α, and granulocyte-macrophage colony-stimulating factor (GM-CSF) (Sojka et al., 2014; Tang et al., 2016), it is possible that LrNK cells might promote Th1 cell polarization under certain conditions. Thus, more work is needed to comprehensively evaluate the functions of LrNK cells in other conditions (such as tumors, autoimmune diseases, and transplant rejection) and in different phases of diseases.

Altogether, these results reveal a PD-L1-dependent immunosuppressive function of LrNK cells during viral infection and differential roles of LrNK and cNK cells in the regulation of hepatic T cell responses. Considering the differential compositions of NK cell subsets in different tissues, the results of this study have profound implications for our understanding of the specific features of local immunity.

STAR★METHODS

Detailed methods are provided in the online version of this paper and include the following:

- KEY RESOURCES TABLE
- CONTACT FOR REAGENT AND RESOURCE SHARING
- EXPERIMENTAL MODEL AND SUBJECT DETAILS
  - Mice
- METHOD DETAILS
  - Viruses and infection details
  - Cell isolation

Figure 6. Blockade of PD-L1 on LrNK Cells prior to Adoptive Transfer Abrogates Inhibition of Antiviral T Cell Responses

(A) LrNK and cNK cells (2×10^5) were sorted from $CD45.1^+$ mice and incubated with anti-PD-L1 monoclonal antibody (mAb) prior to adoptive transfer into sub-lethally irradiated $CD45.2^+$ B6 mice. The recipient mice were then infected with LCMV Armstrong and analyzed at PI day 7. Representative plots show gp66-specific $CD4^+$ T cells and gp33-specific $CD8^+$ T cells in the livers of the recipient mice.

(B and C) Ratio (B) and absolute numbers (C) of hepatic gp66-specific $CD4^+$ T cells from the recipient mice in (A).

(D and E) Ratio (D) and absolute numbers (E) of hepatic gp33-specific $CD8^+$ T cells from the recipient mice in (A).

(F and G) Quantification of intracellular IFN-γ staining of hepatic $CD4^+$ T cells (F) and $CD8^+$ T cells (G) from the recipient mice in (A).

(H and I) Viral titers in the livers (H) and serum ALT concentrations (I) from the recipient mice in (A).

(J–N) LrNK and cNK cells were sorted from $CD45.1^+$ mice and incubated with anti-PD-L1 mAb prior to adoptive transfer into sub-lethally irradiated $CD45.2^+$ B6 mice. Recipient mice were then infected with LCMV Armstrong and intraperitoneally (i.p.) injected with 1 mg BrdU at PI day 6. BrdU incorporation and Ki67 staining of hepatic gp66-specific $CD4^+$ T cells and gp33-specific $CD8^+$ T were analyzed at PI day 7. Representative plots (J) and percentages (K–N) are shown.

Data represent two or three independent experiments with three to seven mice per group (mean ± SEM; ns, not significant; *$p < 0.05$, **$p < 0.01$).

See also Figures S6 and S7.

- Antibody staining and flow cytometry
- Cell sorting and transfer
- BrdU incorporation
- Virus titration
- Assay for T cell proliferation *in vitro*
- Microarray analysis and Gene Ontology enrichment analysis
- Histology
- Analysis of liver transaminase activity
- Statistics

SUPPLEMENTAL INFORMATION

Supplemental Information includes seven figures and can be found with the article online at https://doi.org/10.1016/j.immuni.2018.12.024.

ACKNOWLEDGMENTS

We thank Prof. Rafi Ahmed (Emory University School of Medicine, GA, USA) for providing the LCMV strains and the National Institutes of Health Tetramer Core Facility at Emory University for providing the anti-LCMV gp66 tetramer. This work was supported by the National Natural Science Foundation of China (81788101, 91642105, 81571522, 91542114, 81761128013, and 91542000) and the Chinese Academy of Sciences (XDB29030000).

AUTHOR CONTRIBUTIONS

J.Z. designed the research, performed experiments, and drafted the manuscript; H.P. designed the research and wrote the paper; K.L. and K.Q. performed the microarray analysis; B.W. assisted with cell preparation; L.Y., Y.W., and Z.D. assisted with the experimental models; R.S. and H.W. contributed to the discussion; and Z.T. designed the research and wrote the manuscript.

DECLARATION OF INTERESTS

The authors declare no competing interests.

Received: June 25, 2018
Revised: October 25, 2018
Accepted: December 18, 2018
Published: January 29, 2019

REFERENCES

Adam, C., King, S., Allgeier, T., Braumüller, H., Lüking, C., Mysliwietz, J., Kriegeskorte, A., Busch, D.H., Röcken, M., and Mocikat, R. (2005). DC-NK cell cross talk as a novel CD4+ T-cell-independent pathway for antitumor CTL induction. Blood *106*, 338–344.

Ahn, E., Araki, K., Hashimoto, M., Li, W., Riley, J.L., Cheung, J., Sharpe, A.H., Freeman, G.J., Irving, B.A., and Ahmed, R. (2018). Role of PD-1 during effector CD8 T cell differentiation. Proc. Natl. Acad. Sci. USA *115*, 4749–4754.

Artis, D., and Spits, H. (2015). The biology of innate lymphoid cells. Nature *517*, 293–301.

Aw Yeang, H.X., Piersma, S.J., Lin, Y., Yang, L., Malkova, O.N., Miner, C., Krupnick, A.S., Chapman, W.C., and Yokoyama, W.M. (2017). Cutting edge: human CD49e- NK cells are tissue resident in the liver. J. Immunol. *198*, 1417–1422.

Barber, D.L., Wherry, E.J., Masopust, D., Zhu, B., Allison, J.P., Sharpe, A.H., Freeman, G.J., and Ahmed, R. (2006). Restoring function in exhausted CD8 T cells during chronic viral infection. Nature *439*, 682–687.

Bauché, D., Joyce-Shaikh, B., Jain, R., Grein, J., Ku, K.S., Blumenschein, W.M., Ganal-Vonarburg, S.C., Wilson, D.C., McClanahan, T.K., Malefyt, R.W., et al. (2018). LAG3^{+} regulatory T cells restrain interleukin-23-producing cx3cr1^{+} gut-resident macrophages during group 3 innate lymphoid cell-driven colitis. Immunity *49*, 342–352.e5.

Bukowski, J.F., Woda, B.A., Habu, S., Okumura, K., and Welsh, R.M. (1983). Natural killer cell depletion enhances virus synthesis and virus-induced hepatitis in vivo. J. Immunol. *131*, 1531–1538.

Cerboni, C., Zingoni, A., Cippitelli, M., Piccoli, M., Frati, L., and Santoni, A. (2007). Antigen-activated human T lymphocytes express cell-surface NKG2D ligands via an ATM/ATR-dependent mechanism and become susceptible to autologous NK- cell lysis. Blood *110*, 606–615.

Constantinides, M.G., McDonald, B.D., Verhoef, P.A., and Bendelac, A. (2014). A committed precursor to innate lymphoid cells. Nature *508*, 397–401.

Cook, K.D., and Whitmire, J.K. (2013). The depletion of NK cells prevents T cell exhaustion to efficiently control disseminating virus infection. J. Immunol. *190*, 641–649.

Cortez, V.S., Ulland, T.K., Cervantes-Barragan, L., Bando, J.K., Robinette, M.L., Wang, Q., White, A.J., Gilfillan, S., Cella, M., and Colonna, M. (2017). SMAD4 impedes the conversion of NK cells into ILC1-like cells by curtailing non-canonical TGF-β signaling. Nat. Immunol. *18*, 995–1003.

Crispe, I.N. (2009). The liver as a lymphoid organ. Annu. Rev. Immunol. *27*, 147–163.

Crome, S.Q., Lang, P.A., Lang, K.S., and Ohashi, P.S. (2013). Natural killer cells regulate diverse T cell responses. Trends Immunol. *34*, 342–349.

Crome, S.Q., Nguyen, L.T., Lopez-Verges, S., Yang, S.Y., Martin, B., Yam, J.Y., Johnson, D.J., Nie, J., Pniak, M., Yen, P.H., et al. (2017). A distinct innate lymphoid cell population regulates tumor-associated T cells. Nat. Med. *23*, 368–375.

Cuff, A.O., Robertson, F.P., Stegmann, K.A., Pallett, L.J., Maini, M.K., Davidson, B.R., and Male, V. (2016). Eomeshi NK cells in human liver are long-lived and do not recirculate but can be replenished from the circulation. J. Immunol. *197*, 4283–4291.

Cunningham, E.C., Sharland, A.F., and Bishop, G.A. (2013). Liver transplant tolerance and its application to the clinic: can we exploit the high dose effect? Clin. Dev. Immunol. *2013*, 419692.

Deaglio, S., Dwyer, K.M., Gao, W., Friedman, D., Usheva, A., Erat, A., Chen, J.F., Enjyoji, K., Linden, J., Oukka, M., et al. (2007). Adenosine generation catalyzed by CD39 and CD73 expressed on regulatory T cells mediates immune suppression. J. Exp. Med. *204*, 1257–1265.

Deniz, G., Erten, G., Kücüksezer, U.C., Kocacik, D., Karagiannidis, C., Aktas, E., Akdis, C.A., and Akdis, M. (2008). Regulatory NK cells suppress antigen-specific T cell responses. J. Immunol. *180*, 850–857.

Dong, H., Zhu, G., Tamada, K., Flies, D.B., van Deursen, J.M., and Chen, L. (2004). B7-H1 determines accumulation and deletion of intrahepatic CD8(+) T lymphocytes. Immunity *20*, 327–336.

Fu, B., Li, X., Sun, R., Tong, X., Ling, B., Tian, Z., and Wei, H. (2013). Natural killer cells promote immune tolerance by regulating inflammatory TH17 cells at the human maternal-fetal interface. Proc. Natl. Acad. Sci. USA *110*, E231–E240.

Gao, B. (2016). Basic liver immunology. Cell. Mol. Immunol. *13*, 265–266.

Gao, Y., Souza-Fonseca-Guimaraes, F., Bald, T., Ng, S.S., Young, A., Ngiow, S.F., Rautela, J., Straube, J., Waddell, N., Blake, S.J., et al. (2017). Tumor immunoevasion by the conversion of effector NK cells into type 1 innate lymphoid cells. Nat. Immunol. *18*, 1004–1015.

Geiger, T.L., Abt, M.C., Gasteiger, G., Firth, M.A., O'Connor, M.H., Geary, C.D., O'Sullivan, T.E., van den Brink, M.R., Pamer, E.G., Hanash, A.M., and Sun, J.C. (2014). Nfil3 is crucial for development of innate lymphoid cells and host protection against intestinal pathogens. J. Exp. Med. *211*, 1723–1731.

Gerosa, F., Baldani-Guerra, B., Nisii, C., Marchesini, V., Carra, G., and Trinchieri, G. (2002). Reciprocal activating interaction between natural killer cells and dendritic cells. J. Exp. Med. *195*, 327–333.

Gordon, S.M., Chaix, J., Rupp, L.J., Wu, J., Madera, S., Sun, J.C., Lindsten, T., and Reiner, S.L. (2012). The transcription factors T-bet and Eomes control key checkpoints of natural killer cell maturation. Immunity *36*, 55–67.

Gu, J., Ni, X., Pan, X., Lu, H., Lu, Y., Zhao, J., Guo Zheng, S., Hippen, K.L., Wang, X., and Lu, L. (2017). Human CD39^{hi} regulatory T cells present stronger

stability and function under inflammatory conditions. Cell. Mol. Immunol. *14*, 521–528.

Harmon, C., Robinson, M.W., Fahey, R., Whelan, S., Houlihan, D.D., Geoghegan, J., and O'Farrelly, C. (2016). Tissue-resident Eomes(hi) T-bet(lo) CD56(bright) NK cells with reduced proinflammatory potential are enriched in the adult human liver. Eur. J. Immunol. *46*, 2111–2120.

Hepworth, M.R., Monticelli, L.A., Fung, T.C., Ziegler, C.G., Grunberg, S., Sinha, R., Mantegazza, A.R., Ma, H.L., Crawford, A., Angelosanto, J.M., et al. (2013). Innate lymphoid cells regulate CD4+ T-cell responses to intestinal commensal bacteria. Nature *498*, 113–117.

Huang, C.T., Workman, C.J., Flies, D., Pan, X., Marson, A.L., Zhou, G., Hipkiss, E.L., Ravi, S., Kowalski, J., Levitsky, H.I., et al. (2004). Role of LAG-3 in regulatory T cells. Immunity *21*, 503–513.

Iwai, Y., Terawaki, S., Ikegawa, M., Okazaki, T., and Honjo, T. (2003). PD-1 inhibits antiviral immunity at the effector phase in the liver. J. Exp. Med. *198*, 39–50.

Klose, C.S.N., Flach, M., Möhle, L., Rogell, L., Hoyler, T., Ebert, K., Fabiunke, C., Pfeifer, D., Sexl, V., Fonseca-Pereira, D., et al. (2014). Differentiation of type 1 ILCs from a common progenitor to all helper-like innate lymphoid cell lineages. Cell *157*, 340–356.

Krueger, P.D., Narayanan, S., Surette, F.A., Brown, M.G., Sung, S.J., and Hahn, Y.S. (2017). Murine liver-resident group 1 innate lymphoid cells regulate optimal priming of anti-viral CD8+ T cells. J. Leukoc. Biol. *101*, 329–338.

Lam, V.C., and Lanier, L.L. (2017). NK cells in host responses to viral infections. Curr. Opin. Immunol. *44*, 43–51.

Lang, P.A., Lang, K.S., Xu, H.C., Grusdat, M., Parish, I.A., Recher, M., Elford, A.R., Dhanji, S., Shaabani, N., Tran, C.W., et al. (2012). Natural killer cell activation enhances immune pathology and promotes chronic infection by limiting CD8+ T-cell immunity. Proc. Natl. Acad. Sci. USA *109*, 1210–1215.

Laouar, Y., Sutterwala, F.S., Gorelik, L., and Flavell, R.A. (2005). Transforming growth factor-beta controls T helper type 1 cell development through regulation of natural killer cell interferon-gamma. Nat. Immunol. *6*, 600–607.

Lee, S.H., Kim, K.S., Fodil-Cornu, N., Vidal, S.M., and Biron, C.A. (2009). Activating receptors promote NK cell expansion for maintenance, IL-10 production, and CD8 T cell regulation during viral infection. J. Exp. Med. *206*, 2235–2251.

Li, F., and Tian, Z. (2013). The liver works as a school to educate regulatory immune cells. Cell. Mol. Immunol. *10*, 292–302.

Li, F., Wei, H., Wei, H., Gao, Y., Xu, L., Yin, W., Sun, R., and Tian, Z. (2013). Blocking the natural killer cell inhibitory receptor NKG2A increases activity of human natural killer cells and clears hepatitis B virus infection in mice. Gastroenterology *144*, 392–401.

Liang, Y., Jie, Z., Hou, L., Yi, P., Wang, W., Kwota, Z., Salvato, M., de Waal Malefyt, R., Soong, L., and Sun, J. (2015). IL-33 promotes innate IFN-γ production and modulates dendritic cell response in LCMV-induced hepatitis in mice. Eur. J. Immunol. *45*, 3052–3063.

Limmer, A., Ohl, J., Kurts, C., Ljunggren, H.G., Reiss, Y., Groettrup, M., Momburg, F., Arnold, B., and Knolle, P.A. (2000). Efficient presentation of exogenous antigen by liver endothelial cells to CD8+ T cells results in antigen-specific T-cell tolerance. Nat. Med. *6*, 1348–1354.

Liu, Z.X., Govindarajan, S., Okamoto, S., and Dennert, G. (2000). NK cells cause liver injury and facilitate the induction of T cell-mediated immunity to a viral liver infection. J. Immunol. *164*, 6480–6486.

Mackay, L.K., Minnich, M., Kragten, N.A., Liao, Y., Nota, B., Seillet, C., Zaid, A., Man, K., Preston, S., Freestone, D., et al. (2016). Hobit and Blimp1 instruct a universal transcriptional program of tissue residency in lymphocytes. Science *352*, 459–463.

Martín-Fontecha, A., Thomsen, L.L., Brett, S., Gerard, C., Lipp, M., Lanzavecchia, A., and Sallusto, F. (2004). Induced recruitment of NK cells to lymph nodes provides IFN-gamma for T(H)1 priming. Nat. Immunol. *5*, 1260–1265.

McCausland, M.M., and Crotty, S. (2008). Quantitative PCR technique for detecting lymphocytic choriomeningitis virus in vivo. J. Virol. Methods *147*, 167–176.

McIntyre, K.W., and Welsh, R.M. (1986). Accumulation of natural killer and cytotoxic T large granular lymphocytes in the liver during virus infection. J. Exp. Med. *164*, 1667–1681.

Mehrotra, P.T., Donnelly, R.P., Wong, S., Kanegane, H., Geremew, A., Mostowski, H.S., Furuke, K., Siegel, J.P., and Bloom, E.T. (1998). Production of IL-10 by human natural killer cells stimulated with IL-2 and/or IL-12. J. Immunol. *160*, 2637–2644.

Mocikat, R., Braumüller, H., Gumy, A., Egeter, O., Ziegler, H., Reusch, U., Bubeck, A., Louis, J., Mailhammer, R., Riethmüller, G., et al. (2003). Natural killer cells activated by MHC class I(low) targets prime dendritic cells to induce protective CD8 T cell responses. Immunity *19*, 561–569.

Mueller, S.N., Vanguri, V.K., Ha, S.J., West, E.E., Keir, M.E., Glickman, J.N., Sharpe, A.H., and Ahmed, R. (2010). PD-L1 has distinct functions in hematopoietic and nonhematopoietic cells in regulating T cell responses during chronic infection in mice. J. Clin. Invest. *120*, 2508–2515.

Penaloza-MacMaster, P., Kamphorst, A.O., Wieland, A., Araki, K., Iyer, S.S., West, E.E., O'Mara, L., Yang, S., Konieczny, B.T., Sharpe, A.H., et al. (2014). Interplay between regulatory T cells and PD-1 in modulating T cell exhaustion and viral control during chronic LCMV infection. J. Exp. Med. *211*, 1905–1918.

Peng, H., and Sun, R. (2017). Liver-resident NK cells and their potential functions. Cell. Mol. Immunol. *14*, 890.

Peng, H., and Tian, Z. (2017). Diversity of tissue-resident NK cells. Semin. Immunol. *31*, 3–10.

Peng, H., Jiang, X., Chen, Y., Sojka, D.K., Wei, H., Gao, X., Sun, R., Yokoyama, W.M., and Tian, Z. (2013). Liver-resident NK cells confer adaptive immunity in skin-contact inflammation. J. Clin. Invest. *123*, 1444–1456.

Peng, H., Wisse, E., and Tian, Z. (2016). Liver natural killer cells: subsets and roles in liver immunity. Cell. Mol. Immunol. *13*, 328–336.

Peppa, D., Gill, U.S., Reynolds, G., Easom, N.J., Pallett, L.J., Schurich, A., Micco, L., Nebbia, G., Singh, H.D., Adams, D.H., et al. (2013). Up-regulation of a death receptor renders antiviral T cells susceptible to NK cell-mediated deletion. J. Exp. Med. *210*, 99–114.

Protzer, U., Maini, M.K., and Knolle, P.A. (2012). Living in the liver: hepatic infections. Nat. Rev. Immunol. *12*, 201–213.

Rabinovich, B.A., Li, J., Shannon, J., Hurren, R., Chalupny, J., Cosman, D., and Miller, R.G. (2003). Activated, but not resting, T cells can be recognized and killed by syngeneic NK cells. J. Immunol. *170*, 3572–3576.

Raziorrouh, B., Ulsenheimer, A., Schraut, W., Heeg, M., Kurktschiev, P., Zachoval, R., Jung, M.C., Thimme, R., Neumann-Haefelin, C., Horster, S., et al. (2011). Inhibitory molecules that regulate expansion and restoration of HCV-specific CD4+ T cells in patients with chronic infection. Gastroenterology *141*, 1422–1431, 1431.e1–1431.e6.

Schildberg, F.A., Klein, S.R., Freeman, G.J., and Sharpe, A.H. (2016). Coinhibitory Pathways in the B7-CD28 ligand-receptor family. Immunity *44*, 955–972.

Schuster, I.S., Wikstrom, M.E., Brizard, G., Coudert, J.D., Estcourt, M.J., Manzur, M., O'Reilly, L.A., Smyth, M.J., Trapani, J.A., Hill, G.R., et al. (2014). TRAIL+ NK cells control CD4+ T cell responses during chronic viral infection to limit autoimmunity. Immunity *41*, 646–656.

Schuster, I.S., Coudert, J.D., Andoniou, C.E., and Degli-Esposti, M.A. (2016). "Natural regulators": NK cells as modulators of T cell immunity. Front. Immunol. *7*, 235.

Schwartz, C., Khan, A.R., Floudas, A., Saunders, S.P., Hams, E., Rodewald, H.R., McKenzie, A.N.J., and Fallon, P.G. (2017). ILC2s regulate adaptive Th2 cell functions via PD-L1 checkpoint control. J. Exp. Med. *214*, 2507–2521.

Seillet, C., Rankin, L.C., Groom, J.R., Mielke, L.A., Tellier, J., Chopin, M., Huntington, N.D., Belz, G.T., and Carotta, S. (2014). Nfil3 is required for the development of all innate lymphoid cell subsets. J. Exp. Med. *211*, 1733–1740.

Seillet, C., Belz, G.T., and Huntington, N.D. (2016). Development, homeostasis, and heterogeneity of NK Cells and ILC1. Curr. Top. Microbiol. Immunol. *395*, 37–61.

Soderquest, K., Powell, N., Luci, C., van Rooijen, N., Hidalgo, A., Geissmann, F., Walzer, T., Lord, G.M., and Martín-Fontecha, A. (2011). Monocytes control natural killer cell differentiation to effector phenotypes. Blood *117*, 4511–4518.

Sojka, D.K., Plougastel-Douglas, B., Yang, L., Pak-Wittel, M.A., Artyomov, M.N., Ivanova, Y., Zhong, C., Chase, J.M., Rothman, P.B., Yu, J., et al. (2014). Tissue-resident natural killer (NK) cells are cell lineages distinct from thymic and conventional splenic NK cells. eLife *3*, e01659.

Spits, H., Bernink, J.H., and Lanier, L. (2016). NK cells and type 1 innate lymphoid cells: partners in host defense. Nat. Immunol. *17*, 758–764.

Stegmann, K.A., Robertson, F., Hansi, N., Gill, U., Pallant, C., Christophides, T., Pallett, L.J., Peppa, D., Dunn, C., Fusai, G., et al. (2016). CXCR6 marks a novel subset of T-bet(lo)Eomes(hi) natural killer cells residing in human liver. Sci. Rep. *6*, 26157.

Tang, L., Peng, H., Zhou, J., Chen, Y., Wei, H., Sun, R., Yokoyama, W.M., and Tian, Z. (2016). Differential phenotypic and functional properties of liver-resident NK cells and mucosal ILC1s. J. Autoimmun. *67*, 29–35.

Tiegs, G., and Lohse, A.W. (2010). Immune tolerance: what is unique about the liver. J. Autoimmun. *34*, 1–6.

Townsend, M.J., Weinmann, A.S., Matsuda, J.L., Salomon, R., Farnham, P.J., Biron, C.A., Gapin, L., and Glimcher, L.H. (2004). T-bet regulates the terminal maturation and homeostasis of NK and Valpha14i NKT cells. Immunity *20*, 477–494.

Urbani, S., Amadei, B., Tola, D., Pedrazzi, G., Sacchelli, L., Cavallo, M.C., Orlandini, A., Missale, G., and Ferrari, C. (2008). Restoration of HCV-specific T cell functions by PD-1/PD-L1 blockade in HCV infection: effect of viremia levels and antiviral treatment. J. Hepatol. *48*, 548–558.

Vivier, E., Tomasello, E., Baratin, M., Walzer, T., and Ugolini, S. (2008). Functions of natural killer cells. Nat. Immunol. *9*, 503–510.

Waggoner, S.N., Taniguchi, R.T., Mathew, P.A., Kumar, V., and Welsh, R.M. (2010). Absence of mouse 2B4 promotes NK cell-mediated killing of activated CD8+ T cells, leading to prolonged viral persistence and altered pathogenesis. J. Clin. Invest. *120*, 1925–1938.

Waggoner, S.N., Cornberg, M., Selin, L.K., and Welsh, R.M. (2011). Natural killer cells act as rheostats modulating antiviral T cells. Nature *481*, 394–398.

Wang, J., Sun, R., Wei, H., Dong, Z., Gao, B., and Tian, Z. (2006). Poly I:C prevents T cell-mediated hepatitis via an NK-dependent mechanism. J. Hepatol. *44*, 446–454.

Wang, Y., Li, T., Chen, Y., Wei, H., Sun, R., and Tian, Z. (2017). Involvement of NK cells in IL-28B-mediated immunity against influenza virus infection. J. Immunol. *199*, 1012–1020.

Weizman, O.E., Adams, N.M., Schuster, I.S., Krishna, C., Pritykin, Y., Lau, C., Degli-Esposti, M.A., Leslie, C.S., Sun, J.C., and O'Sullivan, T.E. (2017). ILC1 confer early host protection at initial sites of viral infection. Cell *171*, 795–808.e12.

Welsh, R.M., Brubaker, J.O., Vargas-Cortes, M., and O'Donnell, C.L. (1991). Natural killer (NK) cell response to virus infections in mice with severe combined immunodeficiency. The stimulation of NK cells and the NK cell-dependent control of virus infections occur independently of T and B cell function. J. Exp. Med. *173*, 1053–1063.

Zhang, C., Zhang, J., and Tian, Z. (2006). The regulatory effect of natural killer cells: do "NK-reg cells" exist? Cell. Mol. Immunol. *3*, 241–254.

Zhang, Z., Zhang, J.Y., Wherry, E.J., Jin, B., Xu, B., Zou, Z.S., Zhang, S.Y., Li, B.S., Wang, H.F., Wu, H., et al. (2008). Dynamic programmed death 1 expression by virus-specific CD8 T cells correlates with the outcome of acute hepatitis B. Gastroenterology *134*, 1938–1949, 1949.e1–1949.e3.

Zhang, L.H., Shin, J.H., Haggadone, M.D., and Sunwoo, J.B. (2016). The aryl hydrocarbon receptor is required for the maintenance of liver-resident natural killer cells. J. Exp. Med. *213*, 2249–2257.

STAR★METHODS

KEY RESOURCES TABLE

REAGENT or RESOURCE	SOURCE	IDENTIFIER
Antibodies		
Anti-mouse CD4 (RM4-5) BV510	BD Biosciences	Cat# 563106; RRID: AB_2687550
Anti-mouse CD8 (53-6.7) BV510	BD Biosciences	Cat# 563068; RRID: AB_ 2687548
Anti-mouse CD49a (Ha31/8) PE	BD Biosciences	Cat# 562115; RRID: AB_11153117
Anti-mouse CD49a (Ha31/8) PerCP-CY5.5	BD Biosciences	Cat# 564862; RRID: AB_2734135
Anti-mouse CD49a (Ha31/8) Alexa Fluor 647	BD Biosciences	Cat# 562113; RRID: AB_11153312
Anti-mouse CD49a (Ha31/8) BV786	BD Biosciences	Cat# 740919; RRID: AB_2740560
Anti-mouse CD49b (CD49b) PE	BD Biosciences	Cat# 553858; RRID: AB_395094
Anti-mouse CD49b (CD49b) BV421	BD Biosciences	Cat# 563063; RRID: AB_2737983
Anti-mouse CD107a (1D4B) FITC	BD Biosciences	Cat# 553793; RRID: AB_395057
Anti-mouse LAG3 (C9B7W) PE	BD Biosciences	Cat# 552380; RRID: AB_394374
Anti-mouse PD-L1 (MIH5) PE	BD Biosciences	Cat# 558091; RRID: AB_397018
Anti-mouse PD-L2 (TY25) APC	BD Biosciences	Cat# 560086; RRID: AB_1645223
Anti-mouse IFN-γ (XMG1.2) BV786	BD Biosciences	Cat# 563773; RRID: AB_2738419
Anti-mouse CD39 (24DMS2) PE	eBioscience	Cat# 12-0391-82; RRID: AB_1210740
Anti-mouse CD73 (TY/11.8) PE	eBioscience	Cat# 12-0731-82; RRID: AB_763513
Anti-mouse CD73 (TY/11.8) PerCP-eFluor 710	eBioscience	Cat# 46-0739-41
Anti-mouse DR5 (MD5-1) PE	eBioscience	Cat# 12-5883-83; RRID: AB_466000
Anti-mouse Eomes (Dan11mag) 660	eBioscience	Cat# 50-4875-82
Anti-mouse Granzyme B (16G6) PE	eBioscience	Cat# 12-8822-80; RRID: AB_466216
Anti-mouse Ki67 (SolA15) 660	eBioscience	Cat# 50-5698-82
Anti-mouse TRAIL (N2B2) PE	eBioscience	Cat# 12-5951-83; RRID: AB_466058
Anti-mouse Perforin (eBioOMAK-D) APC	eBioscience	Cat# 17-9392-80; RRID: AB_469514
Anti-mouse CD3ε (145-2C11) PE-CY7	BioLegend	Cat# 100320; RRID: AB_312685
Anti-mouse CD3ε (145-2C11) APC-CY7	BioLegend	Cat# 100330; RRID: AB_1877170
Anti-mouse CD4 (RM4-5) FITC	BioLegend	Cat# 100510; RRID: AB_312713
Anti-mouse CD8 (53-6.7) PerCP-Cy5.5	BioLegend	Cat# 100734; RRID: AB_2075238
Anti-mouse CD11b (M1/70) APC-CY7	BioLegend	Cat# 101226; RRID: AB_830642
Anti-mouse CD19 (1D3/CD19) PerCP-Cy5.5	BioLegend	Cat# 115534; RRID: AB_2072925
Anti-mouse CD27 (LG.3A10) APC	BioLegend	Cat#124212; RRID: AB_2073425
Anti-mouse CD45 (30-F11) PE-CY7	BioLegend	Cat# 103114; RRID: AB_312979
Anti-mouse CD45.1 (A20) PE-CY7	BioLegend	Cat# 110730; RRID: AB_1134168
Anti-mouse CD45.2 (104) APC-CY7	BioLegend	Cat# 109824; RRID: AB_830789
Anti-mouse CD200R (OX2R) FITC	BioLegend	Cat# 123910; RRID: AB_2244385
Anti-mouse CD200R (OX2R) PE	BioLegend	Cat# 123908; RRID: AB_2074080
Anti-mouse ICOSL (HK5.3) PE	BioLegend	Cat# 107405; RRID: AB_2248797
Anti-mouse IFN-γ (XMG1.2) PE	BioLegend	Cat# 505808; RRID: AB_315402
Anti-mouse IL-2 (JES7-5H4) PerCP-Cy5.5	BioLegend	Cat# 503822; RRID: AB_2123676
Anti-mouse NK1.1 (PK136) PE-CY7	BioLegend	Cat# 108714; RRID: AB_389364
Anti-mouse NK1.1 (PK136) APC-CY7	BioLegend	Cat# 108724; RRID: AB_830871
Anti-mouse NK1.1 (PK136) BV605	BioLegend	Cat# 108740; RRID: AB_2562274
Anti-mouse NKp46 (29A1.4) PerCP-Cy5.5	BioLegend	Cat# 137610; RRID: AB_10641137
Anti-mouse PD-1 (29F.1A12) APC	BioLegend	Cat# 135210; RRID: AB_2159183
Anti-mouse T-bet (4B10) PE	BioLegend	Cat# 644810; RRID: AB_2200542
Anti-mouse TNF-α (MP6-XT22) PE	BioLegend	Cat# 506306; RRID: AB_315427

(*Continued on next page*)

Continued

REAGENT or RESOURCE	SOURCE	IDENTIFIER
Anti-mouse TNF-α (MP6-XT22) BV421	BioLegend	Cat# 506328; RRID: AB_2562902
Anti-LCMV gp33 tetramer PE	Medical & Biological Laboratories	Cat# TS-M512-1
Anti-LCMV gp33 tetramer APC	Medical & Biological Laboratories	Cat# TS-M512-2
Anti-LCMV gp66 tetramer	National Institutes of Health Tetramer Core Facility	N/A
Bacterial and Virus Strains		
Replication-deficient adenovirus	5 + MMI	N/A
LCMV Armstrong	Rafi Ahmed, Emory University	Grew up in house
LCMV Clone13	Rafi Ahmed, Emory University	Grew up in house
Chemicals, Peptides, and Recombinant Proteins		
Anti-CD3 mAb	BD Biosciences	Cat# 553057; RRID: AB_394590
Anti-CD28 mAb	BD Biosciences	Cat# 553294; RRID: AB_394763
Anti-PD-L1 mAb	BioLegend	Cat# 124304; RRID: AB_961232
Anti-TRAIL mAb	eBioscience	Cat# 16-5951-81; RRID: AB_469163
CFSE	Sigma-Aldrich	Cat# 21888
Recombinant Human IL-2	Jiangsu Kingsley Pharmaceutical Co., Ltd.	Cat# S10970056
Collagenase I	Sigma	Cat# C0130; CAS: 9001-12-1
Percoll	GE Healthcare	Cat# 17089101
TRIzol reagent	Invitrogen	Cat# 15596018
Critical Commercial Assays		
Adeno-X Rapid Titer Kit	Clontech	Cat# 632250
TIANamp Virus RNA Kit	TIANGEN	Cat# DP315-R
ALT diagnostic kit	Rong Sheng	Cat# 360100
FITC BrdU Flow Kit instructions	BD Biosciences	Cat# 557891
FoxP3/Transcription Factor Buffer Set	eBioscience	Cat# 00-5523-00
M-MLV Reverse Transcriptase	Invitrogen	Cat# 28025013
SYBR Premix Ex TaqII	TaKaRa	Cat# RR820
Deposited Data		
Microarray analysis of LrNK and cNK cells	Peng et al., 2013	GEO: GSE43339
Experimental Models: Cell Lines		
HEK293 (Human Embryo Kindney)	Shanghai Cell Bank (Chinese Academy of Sciences, Shanghai, China)	Cat# GNHu43
Experimental Models: Organisms/Strains		
C57BL/6	Shanghai Experimental Animal Center	Stock No: 000664
Tbx21$^{-/-}$ mice	Jackson laboratory	Stock No: 004432
CD45.1^{+} B6.SJL mice	Jackson laboratory	Stock No: 002014
Rag1$^{-/-}$ mice	Model Animal Research Center, Nanjing, China	Stock No: 002404
Rag1$^{-/-}$*Tbx21*$^{-/-}$ mice	This study	N/A
Rag1$^{-/-}$*Tbx21*$^{+/-}$ mice	This study	N/A
Pdcd1$^{-/-}$ mice	Beijing Biocytogen Co., Ltd.	Cat# B-CM-080
Ncr1(NKp46)$^{Cre/+}$*Eomes*$^{fl/fl}$	Tsing Hua University, Beijing, China	Dr. Zhongjun Dong
Oligonucleotides		
Primers for LCMV GP, Forward: CATTCACCTG GACTTTGTCAGACTC, Reverse: GCAACTGCT GTGTTCCCGAAAC	McCausland and Crotty, 2008	N/A
Software and Algorithms		
GraphPad Prism	Graphpad Software, Inc.	https://www.graphpad.com/
FlowJo Software	Tree Star	https://www.flowjo.com

CONTACT FOR REAGENT AND RESOURCE SHARING

Further information and requests for resources and reagents should be directed to and will be fulfilled by the Lead Contact, Zhigang Tian (tzg@ustc.edu.cn).

EXPERIMENTAL MODEL AND SUBJECT DETAILS

Mice

WT C57BL/6 (WT B6) mice were purchased from the Shanghai Experimental Animal Center (Shanghai, China). *Tbx21*$^{-/-}$ (T-bet-deficient) mice and CD45.1^{+} B6.SJL mice were obtained from Jackson Laboratory (Bar Harbor, ME, USA). *Rag1*$^{-/-}$ mice were purchased from the Model Animal Research Center (Nanjing, China), and they were crossed with *Tbx21*$^{-/-}$ mice to obtain *Rag1*$^{-/-}$*Tbx21*$^{-/-}$ and *Rag1*$^{-/-}$*Tbx21*$^{+/-}$ mice. *Pdcd1*$^{-/-}$ (PD-1-deficient) mice were purchased from Beijing Biocytogen Co., Ltd. (Beijing, China). *Ncr1*(NKp46)$^{Cre/+}$*Eomes*$^{fl/fl}$ mice were provided by Zhongjun Dong (Tsing Hua University, Beijing, China). 6–12-week-old male and female mice were used. Mice were sex- and age-matched for individual experiments. All mice were housed in a specific-pathogen-free facility with unrestricted access to food and water in compliance with the guidelines for the use of experimental animals at the University of Science and Technology of China.

METHOD DETAILS

Viruses and infection details

A replication-deficient adenovirus was purchased from 5 + MMI (Beijing, China). Mice were infected with 2 × 10^9 infectious units (ifu) of adenovirus by intravenous (i.v.) injection. The lymphocytic choriomeningitis virus (LCMV) Armstrong and Clone13 strains were generous gifts from Rafi Ahmed (Emory University, GA, USA). Mice were infected intraperitoneally (i.p.) with 2 × 10^5 plaque forming units (PFU) of LCMV Armstrong or i.v. with 2 × 10^6 PFU of LCMV Clone13.

Cell isolation

Isolation of liver mononuclear cells (MNC) and splenocytes was performed as previously described (Wang et al., 2006). Briefly, the livers were removed and pressed through a 200-gauge mesh, and liver MNCs were collected following 40%–70% percoll density gradient centrifugation. The spleens were also removed and pressed through a 200-gauge mesh. Splenic single-cell leukocyte suspensions were prepared by lysing the erythrocytes with red cell lysis buffer. Isolation of lung lymphocytes was conducted as described previously (Wang et al., 2017). Briefly, the lung was cut into pieces and incubated at 37°C for 60 min in Roswell Park Memorial Institute (RPMI) 1640 medium (Hyclone, South Logan, UT, USA) with 0.1% collagenase I and 5% fetal calf serum (FCS). The supernatant was collected and the lymphocytes were purified by Percoll gradient centrifugation.

Antibody staining and flow cytometry

Monoclonal antibodies (mAbs) against CD4 (RM4-5), CD8 (53-6.7), CD49a (Ha31/8), CD49b (CD49b), CD107a (1D4B), LAG3 (C9B7W), PD-L1 (MIH5), PD-L2 (TY25), and IFN-γ (XMG1.2) were purchased from BD Biosciences (San Jose, CA, USA). Abs against CD39 (24DMS2), CD73 (TY/11.8), DR5 (MD5-1), Eomes (Dan11mag), Granzyme B (16G6), Ki67 (SolA15), TRAIL (N2B2), and Perforin (eBioOMAK-D) were purchased from eBioscience (San Diego, CA, USA). Abs against CD3ε (145-2C11), CD4 (RM4-5), CD8 (53-6.7), CD11b (M1/70), CD19 (1D3/CD19), CD27 (LG.3A10), CD45 (30-F11), CD45.1 (A20), CD45.2 (104), CD200R (OX-110), ICOSL (HK5.3), IFN-γ (XMG1.2), IL-2 (JES7-5H4), NK1.1 (PK136), NKp46 (29A1.4), PD-1 (29F.1A12), T-bet (4B10), and TNF-α (MP6-XT22) were purchased from BioLegend (San Diego, CA, USA). The anti-LCMV gp33 tetramer was purchased from Medical & Biological Laboratories (Nagoya, Japan). The anti-LCMV gp66 tetramer was provided by the National Institutes of Health Tetramer Core Facility (Emory University, GA, USA). The isolated cells were incubated with rat serum to block Fc receptors followed by staining with fluorescently labeled mAbs against surface molecules. For intracellular cytokine staining, cells were stimulated with 30 ng/mL phorbol myristate acetate (PMA; Sigma-Aldrich, St. Louis, MO, USA) and 1 μg/mL ionomycin (Sigma-Aldrich) for 4 h, and 2 μg/mL monensin (Sigma-Aldrich) was added at the beginning of stimulation. After surface staining, cells were fixed, permeabilized (using a FoxP3/Transcription Factor Buffer Set; eBioscience), and then stained with mAbs against the intracellular molecules. All data were collected using a flow cytometer (LSR II and LSRFortessa X-20; BD Biosciences) and analyzed with FlowJo software (Tree Star, Ashland, OR, USA).

Cell sorting and transfer

A FACS Aria cell sorter (BD Biosciences) was used to purify T cells (CD3^{+}NK1.1^{-}), LrNK cells (CD3^{-}CD19^{-}NK1.1^{+}CD49a^{+}CD49b^{-}), cNK cells (CD3^{-}CD19^{-}NK1.1^{+}CD49a^{-}CD49b^{+}), and CD11b^{+}CD27^{-} cNK cells (CD3^{-}CD19^{-}NK1.1^{+}CD49a^{-}CD49b^{+}CD11b^{+}CD27^{-}). The purity of the sorted cell populations was > 95%, as verified by post-sort flow cytometry. For *in vivo* study, purified cells were transferred into sublethally irradiated (5 Gy given 1 day before adoptive transfer) recipient mice, which were then infected with LCMV or adenovirus and assessed at 7 or 14 days post infection.

BrdU incorporation

Mice were i.p. injected with 1 mg BrdU 1 day before harvest. BrdU staining was performed according to the FITC BrdU Flow Kit (BD Biosciences) instructions.

Virus titration

The titers of adenovirus in tissue samples were determined using an Adeno-X Rapid Titer Kit (Clontech, Mountain View, CA, USA) according to the manufacturer's instructions. Briefly, partial tissues from livers were weighed and homogenized in 1ml DMEM medium (Hyclone, South Logan, UT, USA). 10-fold serial dilutions of the tissue homogenate were plated on HEK293 cells in 12-well plates. After incubating the cells at 37°C in 5% CO_2 for 48 hours, the supernatant was aspirated and cells were fixed with ice-cold 100% methanol, followed by staining with mouse anti-adenovirus Hexon antibody (Clontech) and horseradish peroxidase (HRP) conjugated rat anti-mouse antibody (Clontech) as secondary antibody. Then the cells were stained with 3, 3′ diaminobenzidine tetrahydrochloride (DAB) substrate (Clontech), and positively stained cells were counted using a microscope and infectious units (ifu) were calculated.

The LCMV viral loads in tissue samples were quantified using a quantitative real-time polymerase chain reaction (qPCR) assay, as described previously (McCausland and Crotty, 2008). Briefly, partial tissues from livers, spleens and lungs were weighed and homogenized in 1 mL TRIzol reagent (Invitrogen). Virus RNA was isolated using TIANamp Virus RNA Kit (QIAGEN). cDNA synthesis was done using M-MLV Reverse Transcriptase (Invitrogen) and qPCR assays were carried out using SYBR Premix Ex Taq (TaKaRa). LCMV RNA was detected using primers specific for LCMV GP (Forward: CATTCACCTGGACTTTGTCAGACTC, Reverse: GCAACTGCTGTGTTCCCGAAAC). Viral titers were determined by comparing Cq values to a standard curve of an LCMV sample of known concentration.

Assay for T cell proliferation *in vitro*

T cells ($CD3^+NK1.1^-$) from WT B6 mice were sorted and labeled with 2.5 μM carboxyfluorescein diacetate succinimidyl ester (CFSE; Sigma-Aldrich) for 10 min at 37°C. The CFSE-labeled T cells were cultured for 3 days in the presence of anti-CD3 mAb (3 μg/mL; BD Biosciences), anti-CD28 mAb (2 μg/mL; BD Biosciences), and IL-2 (100 IU/mL), with or without purified LrNK or cNK cells at a ratio of T cells-to-NK cells of 3:1 (1×10^5 NK cells at 200 μl/well). The cells were then harvested, and the proliferation of T cells was determined and analyzed by CFSE dilution. The percentage of inhibition was calculated as follows: percentage of inhibition (%) = (control proliferation - sample proliferation)/control proliferation × 100, where sample and control proliferation is the cell proliferation in the presence and absence of NK cells, respectively. A Transwell system (0.4-μm pore size) was used with a T and LrNK cell co-culture system to inhibit cell–cell contact. For the *in vitro* blocking assay, 10 μg/mL anti-PD-L1 mAb (BioLegend) or anti-TRAIL mAb (eBioscience) was added to the co-culture system. For the *ex vivo* blocking assay, 10 μg/mL anti-PD-L1 mAb (BioLegend) was incubated with NK cells prior to adoptive transfer into mice.

Microarray analysis and Gene Ontology enrichment analysis

We used previously published data (accession number: GSE43339) (Peng et al., 2013) for a microarray analysis and a Gene Ontology enrichment analysis. The data were normalized using an R package called RMA, and the DAVID database was used for the Gene Ontology enrichment analysis.

Histology

The liver tissues were fixed in 10% neutral buffered formalin and embedded in paraffin. Thereafter, 6-μm tissue sections were cut and stained with hematoxylin and eosin.

Analysis of liver transaminase activity

Liver injury was assessed based on alanine aminotransferase (ALT) concentrations, which were measured using a commercially available diagnostic kit (Rong Sheng, Shanghai, China) with a Bio-Chemical Analyzer (Rayto, Shenzhen, China).

Statistics

Unpaired Student's t tests were used to compare pairs of groups, and one-way analysis of variance (ANOVA) was used when there were more than two groups. All data are presented as the mean ± standard error of the mean (SEM). Values of $p < 0.05$ were considered statistically significant.